Figure 16. Micronucleus test with bone marrow in B6C3F$_1$ *gpt* delta female mice treated with Furan for 4 weeks

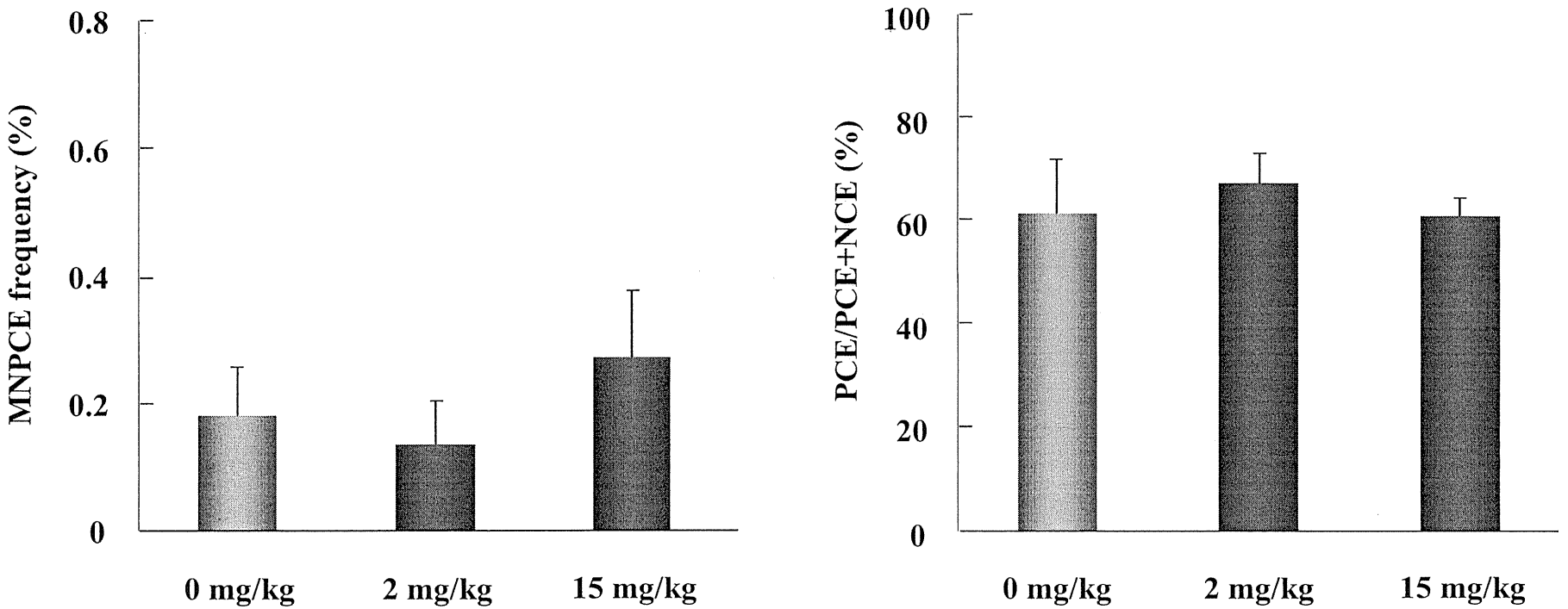

MNPCE : Micronucleated polychromatic erythrocytes, PCE : Polychromatic erythrocytes, NCE : Normochromatic erythrocytes

Figure 17. Micronucleus test with bone marrow in B6C3F$_1$ *gpt* delta male mice treated with Furan for 13 weeks

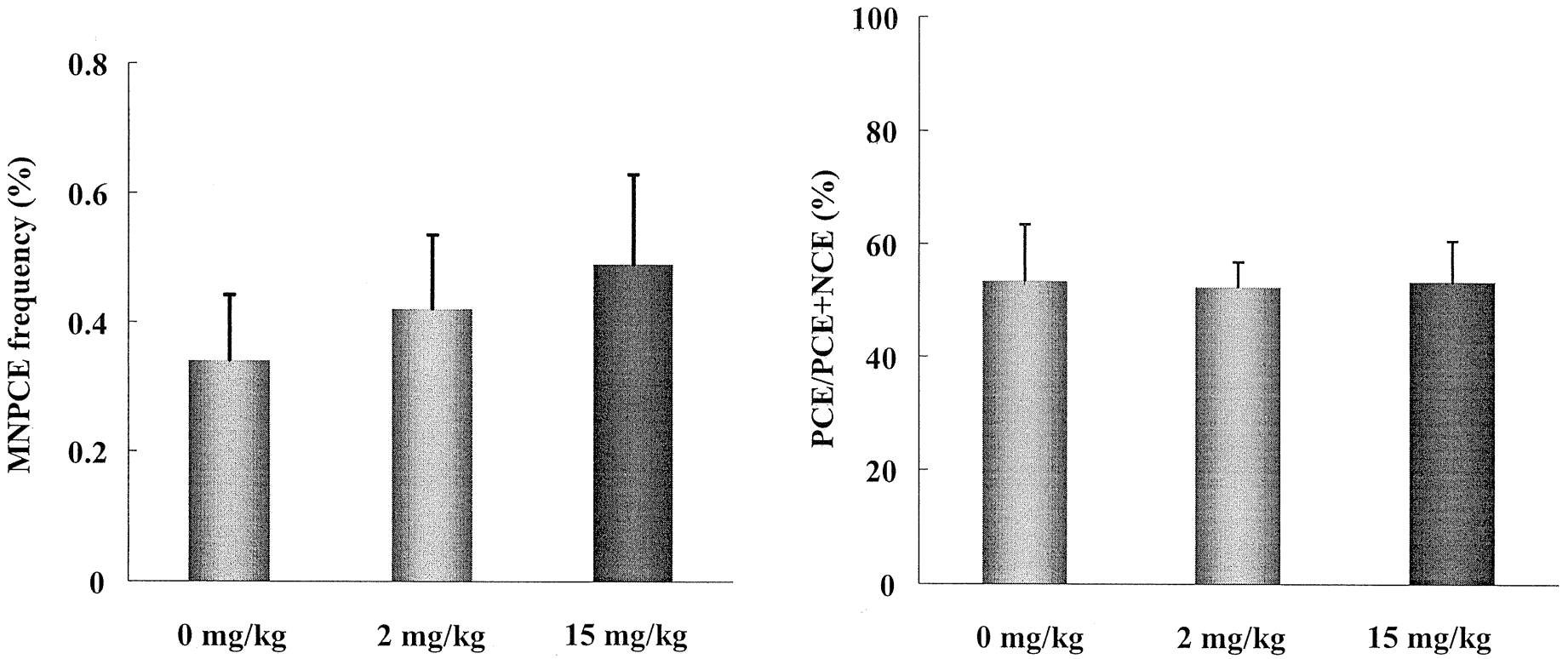

MNPCE : Micronucleated polychromatic erythrocytes, PCE : Polychromatic erythrocytes, NCE : Normochromatic erythrocytes

別紙４

研究成果の刊行に関する一覧表

雑誌

発表者氏名	論文タイトル名	発表誌名	巻号	ページ	出版年
M. Jin, A. Kijima, Y. Suzuki, D. Hibi, T. Inoue, Y. Ishii, T. Nohmi, A. Nishikawa, K.Ogawa, T. Umemura	*In vivo* genotoxicity of 1-methylnaphthalene from comprehensive toxicity studies with B6C3F$_1$ *gpt* delta mice.	J. Toxicol. Sci.			inpress
Suzuki Y, Umemura T, Hibi D, Inoue T, Jin M, Ishii Y, Sakai H, Nohmi T, Yanai T, Nishikawa A, Ogawa K.	Possible involvement of genotoxic mechanisms in estragole-induced hepatocarcinogenesis in rats.	Arch Toxicol.			inpress
Ishii Y, Inoue K, Takasu S, Jin M, Matsushita K, Kuroda K, Fukuhara K, Nishikawa A, Umemura T.	Determination of Lucidin-Specific DNA Adducts by Liquid Chromatography with Tandem Mass Spectrometry in the Livers and Kidneys of Rats Given Lucidin-3-O-pri	Chem Res Toxicol.	25 (5)	1112-1118	2012
Jin M, Kijima A, Suzuki Y, Hibi D, Inoue T, Ishii Y, Nohmi T, Nishikawa A,Ogawa K, Umemura T.	Comprehensive toxicity study of safrole using a medium-terma nimal model with gpt delta rats.	Toxicology	290 (2-3)	312-21	2011
Ishii Y, Suzuki Y, Hibi D, Jin M, Fukuhara K, Umemura T, Nishikawa A.	Detection and quantification of specific DNA adducts by liquid chromatography-tandem mass spectrometry in the livers of rats given estragole at the carcinogenic dose.	Chem Res Toxicol.	24 (4)	532-541	2012

研究成果の刊行物・別刷

Chemical Research in Toxicology

Article

pubs.acs.org/crt

Determination of Lucidin-Specific DNA Adducts by Liquid Chromatography with Tandem Mass Spectrometry in the Livers and Kidneys of Rats Given Lucidin-3-*O*-primeveroside

Yuji Ishii,*[,†] Kaoru Inoue,[†] Shinji Takasu,[†] Meilan Jin,[†] Kohei Matsushita,[†] Ken Kuroda,[†] Kiyoshi Fukuhara,[‡] Akiyoshi Nishikawa,[§] and Takashi Umemura[†]

[†]Division of Pathology, [‡]Division of Organic Chemistry, and [§]Biological Safety Research Center, National Institute of Health Sciences, 1-18-1 Kamiyoga, Setagaya-ku, Tokyo 158-8501, Japan

ABSTRACT: Lucidin-3-*O*-primeveroside (LuP) is a component of madder color (MC), a compound which is carcinogenic in the kidney and liver of rats. Since LuP is metabolized to generate genotoxic compounds such as lucidin (Luc) and rubiadin, it is likely that these play key roles in MC carcinogenesis. In fact, after incubation of Luc with calf thymus DNA, Luc-N^2-dG and N^6-dA adducts were reportedly formed, possibly via the sulfotransferase metabolic pathway. However, the precise extent of formation *in vivo* remains uncertain. In the present study, to quantitatively determine Luc-specific DNA adducts in *in vivo* samples, we developed an online sample purification method using column-switching and an isotope dilution LC-ESI-MS/MS technique. The limits of quantification were 0.2 and 0.04 fmol on column for Luc-N^2-dG and N^6-dA adducts, respectively. Using the new analytical method, we attempted to measure adduct levels in the kidneys and livers of rats treated with 0.06, 0.3, and 1.5% LuP in the diet for one week. Luc-N^2-dG and N^6-dA adducts in these organs were detected at ranges from 7.97 to 51.67/10^9 dG and from1.83 to 37.10/10^9 dA, respectively. Dose-dependent increases of each adduct were observed in both organs. These quantitative data obtained with our newly developed analytical method might help to improve our understanding of MC carcinogenesis.

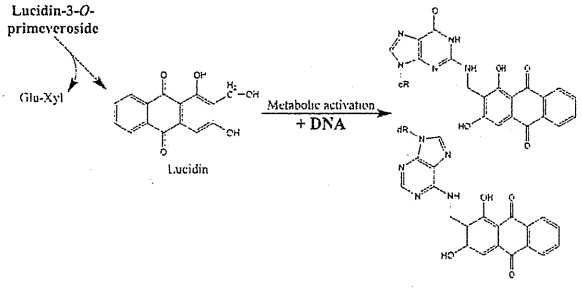

■ INTRODUCTION

Madder color (MC) contains red coloring matter, which has been used for dyeing and widely applied to a variety of foods/drinks in Japan.[1] Our previous study revealed that MC has potent carcinogenicity targeting the kidneys and livers of F344 rats.[2] MC is constituted of many anthraquinone compounds, such as lucidin-3-*O*-primeveroside (LuP), alizarin (Alz), and ruberythric acid. We hypothesized that LuP and its metabolites, lucidin (Luc) and rubiadin (Rub), might take part in MC carcinogenesis because of their genotoxicities.[3−6] In addition, our study clearly demonstrated that Luc and Rub were capable of forming N^2-guanine (N^2-dG) and N^6-adenine (N^6-dA) substitutions *in vitro*, which suggested that Luc and Rub exerted their genotoxicity by metabolic conversion to the ultimate carcinogen, sulfooxy-Luc.[7] However, since actual occurrences of these adduct formations *in vivo* have not been identified, it remains uncertain whether these are responsible for MC carcinogenicity.

The N-2 and N-6 positions of dG or dA are known to be sites susceptible to reaction with electrophiles. In fact, other potent mutagens such as benzo[*a*]pyrene (BP) and 3-nitrobenzanthrone (3-NBA)[8,9] form N^2-dG and N^6-dA adducts that likely play a crucial role in their carcinogenicity.[10−15] In addition, it was found that polκ, one of the translational repair enzymes associated with error-free bypass, exerts its action on bulky N^2-dG adducts.[16] Thus, it is highly probable that Luc-specific DNA adduct formation is an initial step in MC carcinogenesis. Given that modified bases are subject to repair[17] and/or glycoside-bond cleavage,[18] precise quantification of modified bases is important for the investigation of early stages of chemical carcinogenesis.

Liquid chromatography with tandem-mass spectrometry (LC-ESI-MS/MS) is a powerful tool that can achieve high sensitivity and selectivity in the analysis of DNA adducts.[19−21] In the case of accurate quantification of modified bases at extremely low concentrations, the use of stable isotope-labeled standards is necessary to compensate for the loss of analyte during sample preparation, which is the most critical step in eliminating the matrix effect on analysis of modified bases by MS.[22] In this study, we developed a quantitative method for Luc-N^2-dG and N^6-dA adducts in DNA using LC-ESI-MS/MS with a dilution isotope technique. A device for online solid-phase extraction with column switching was also adopted to purify and condense the sample online. After evaluation of applicability to *in vivo* samples, the newly developed LC-ESI-MS/MS method was applied to the quantification of Luc-specific DNA adducts in the kidneys and livers of rats treated with LuP.

Received: February 27, 2012
Published: April 11, 2012

MATERIALS AND METHODS

Caution: *LuP is a mutagen and should be handled accordingly.*

Chemicals and Reagents. LuP was extracted by HPLC from MC (powdered roots of *Rubia tinctorum L.*) used in Japan as a food coloring (San-Ei Gen. F.F.I., Inc., Osaka, Japan).[2] The purity of LuP was 90.5%. It was confirmed by HPLC/UV analysis with a calibration curve of the LuP standard. Alkaline phosphatase, 2′-deoxyguanosine (dG), 2′-deoxyadenosine (dA), phosphodiesterase I from *Crotalus adamanteus* venom (VPDE), and phosphodiesterase II from bovine spleen (SPDE) were purchased from Sigma-Aldrich (St. Louis, MO). Nuclease P1 was obtained from Yamasa Co. (Chiba, Japan). Stable isotope labeled $^{15}N_5$-2′-deoxyguanosine and $^{15}N_5$-2′-deoxyadenosine were obtained from Cambridge Isotope Laboratories (Cambridge, MA). DNA extractor TIS kit was purchased from Wako Pure Chemicals (Tokyo, Japan). All other chemicals used were of specific analytical or HPLC grade. Luc-N^2-dG and N^6-dA adducts and ^{15}N-labeled adducts were synthesized from acetyl-Luc with dG and dA as described in our previous report.[7]

Standard Solutions. Stock solutions (1.0 mM) of Luc-N^2-dG and N^6-dA adducts were prepared in methanol/HPLC grade water (50/50, v/v), respectively. Working solutions for calibration (0.15−7.5 nM for Luc-N^2-dG and 0.03−1.5 nM for Luc-N^6-dA) were prepared by the addition of an adequate amount of ^{15}N-labeled standard and diluting with methanol/HPLC grade water (50/50, v/v) to appropriate concentrations.

Instrumentation. LC-ESI-MS/MS analyses were performed using Quattro Ultima (Micromass) equipped with an ESI source coupled to a Hewlett Packard 1100 series (G1322A, Degasser; G1312A, Bin Pump; G1316A, COLCOM; G1329A, ALS; Agilent technologies, Palo Alto, CA, USA). Two Agilent pumps were used to induce flow to elute the sample from the extraction column. An Intelligent HPLC Pump (JASCO, Tokyo, Japan) was used to induce flow through the extraction column to load and wash the sample and to equilibrate the extraction column. A Wakosil-II C18 (2.0 × 150 mm, 5 μm; Wako Pure Chemicals, Tokyo, Japan) was used for separation. An Inertsil ODS-3 column (4.6 × 50.0 mm, 5.0 μm, GL Sciences Inc., Tokyo, Japan) was used for cleanup and concentration as an extraction column.

CS-LC-MS/MS Conditions. The column-switching system was used for the injection of liquid sample. After 20 μL of the sample was injected with an autosampler, it was loaded onto the extraction column by flowing acetonitrile−0.001% formic acid (15/85, v/v) at a flow rate of 0.5 mL/min using pump C for 5 min. While the extraction column was directed to waste during the 5 min run, the sample was extracted and purified on the online extraction column. The impurities were removed, and Luc-N^2-dG and N^6-dA adducts were retained on the extraction column. After the online extraction for 5 min, the position of the switching valve was changed. This configuration connected the back-flushing extraction column to the analytical column and the MS detector in the flow path of pumps A and B. Solvent A was 0.01% formic acid, and solvent B was 0.01% formic acid-containing acetonitrile. The column was equilibrated with a mixture of solvent A/solvent B (75/25, v/v) at a flow rate of 0.2 mL/min. The column oven was maintained at 40 °C for LC separation. A linear gradient was applied from 25% to 90% acetonitrile at 0 to 20 min, kept at 90% for 10 min, lowered to 25% over 1 min, and equilibrated at the initial conditions for 14 min. After elution for 31 min, the switching valve was returned to its original position. The total run time was 45 min.

LC-ESI-MS/MS Conditions. The mass spectrometer was operated using an ESI source in the positive ion mode (ESI^+) for multiple reaction monitoring (MRM). In the assay for Luc-N^2-dG, the precursor ion ($[M + H]^+$) had a mass of m/z 520, and the selected product ion $[M + H\text{-glycoside-252}]^+$ had a mass of m/z 152. Correspondingly, for $^{15}N_5$-Luc-N^2-dG, the precursor ion had a mass of m/z 525, and the selected product ion had a mass of m/z 157. The cone voltage used was 14 V, and the collision energy was 14 eV. In the assay for Luc-N^6-dA, the precursor ion ($[M + H]^+$) had a mass of m/z 504, and the selected product ion $[M + H\text{-glycoside}]^+$ had a mass of m/z 388. Correspondingly, for $^{15}N_5$- Luc-N^6-dA, the precursor ion had a mass of m/z 509, and the selected product ion had a mass of m/z 393. The cone voltage used was 12 V, and the collision energy was 18 eV. The source block temperature was 150 °C, and the desolvation temperature was 400 °C. The flow rate of the cone gas was set at 200 L/h, while that of the desolvation gas was set at 600 L/h. Under these conditions, the standard retention times were 13.0 and 16.0 min for Luc-N^2-dG and Luc-N^6-dA, respectively.

Validation of LC-MS/MS Analysis. The recovery was evaluated by calculating the mean of the response at each concentration. The spiked concentrations (low, middle, and high doses) of Luc-N^2-dG and Luc-N^6-dA were determined from the concentrations of each adduct in the liver DNA of nontreated rats, using LC-ESI-MS/MS. A standard sample was added together with adequate amount of ^{15}N-labeled standards to 20 mM sodium acetate buffer (pH 4.2) for DNA digestion so that the final concentration could be set to 0.01, 0.5, and 5 nmol/L for Luc-N^2-dG and 0.002, 0.01, and 0.1 nmol/L for Luc-N^6-dA. The extracted DNA pellets of rat liver were redissolved with this buffer and were digested according to the protocol. The sample was analyzed with the LC-ESI-MS/MS method, and the recovery rates were calculated. The interday precision was analyzed using liver samples of three rats treated with 0.3% LuP. Luc-N^2-dG and Luc-N^6-dA analyses were performed on four different days.

Animals and Treatment. The protocol for this study was approved by the Animal Care and Utilization Committee of the National Institute of Health Sciences (Tokyo, Japan). Five-week-old male F344 rats were obtained from Japan Charles River (Shizuoka, Japan). Twenty F344 rats were housed in polycarbonate cages (five rats per cage) with hardwood chips for bedding, using conventional temperature (23 ± 2 °C), humidity (55 ± 5%), air change (12 times per hour), and lighting (12 h light/dark cycle) and were given free access to CRF-1 basal diet (Oriental Yeast Co., Ltd., Tokyo, Japan) and tap water. Starting at six weeks of age, the four groups of five rats were fed a diet containing 0.06, 0.3, or 1.5% LuP or maintained as nontreatment controls for seven days. LuP doses were calculated taking into account LuP purity. All rats were euthanized after seven days by exsanguination under anesthesia, and the kidneys and livers were immediately removed. Samples were frozen with liquid nitrogen and stored at −80 °C until the measurement of Luc-specific DNA adducts.

DNA Isolation and Enzymatic Digestion. DNA extraction and digestion were performed according to the method of Delatour et al.[23] and our previous report.[20] Frozen liver (150 mg) and kidney (80 mg) tissues were used for DNA isolation. The tissue samples were homogenized with lysis buffer included in a DNA extractor TIS kit (Wako Pure Chemicals, Tokyo, Japan). The mixture was centrifuged at 10000*g* for 20 s at 4 °C. The pellet was dissolved in 200 μL of enzyme reaction buffer. After the treatment of RNase and protease K, the DNA pellet was obtained by washing with 2-propanol and ethanol, and centrifugation.

To determine optimal conditions for DNA digestion for Luc-specific DNA adducts, DNA digestion efficiency was compared between two methods using liver samples of rats treated with 0.3% LuP. The dried DNA pellets were dissolved in ^{15}N-labeled standard solution containing 20 mM sodium acetate buffer, pH 4.8, and then digested as follows. In method one, 20 μL of nuclease P1 (2000 U/mL) and 30 μL of water were added and incubated for 6 h at 37 °C. Subsequently, we added 20 μL of 1.0 M Tris-HCl buffer, pH 8.2, and it was incubated with 2 μL of alkaline phosphatase (2500 U/mL) and 10 μL of water for 2 h at 37 °C. In method two, 40 μL of nuclease P1 (2000 U/mL) and 30 μL of SPDE (0.4 U/mL) were added and incubated for 6 h at 37 °C. Subsequently, we added 20 μL of 1.0 M Tris-HCl buffer, pH 8.2, and it was incubated with 4 μL of alkaline phosphatase (2500 U/mL) and 10 μL of VPDE (0.26 U/mL) for 2 h at 37 °C. Two samples digested from identical DNA samples were combined into one sample. For dG and dA analysis, a 50 μL portion of the digested DNA sample was passed through a 100,000 NMWL filter (Millipore, Bedford, MA) and injected into the LC-UV. For adducts analysis, 300 μL of the digested sample was dried in a freeze-dryer and redissolved in 20 μL of water/methanol (50:50, v/v). Samples were injected into the CS-LC-ESI-MS/MS.

dx.doi.org/10.1021/tx300084p | *Chem. Res. Toxicol.* 2012, 25, 1112−1118

LC-UV Analysis for dG and dA. dG and dA were determined with a LC-UV system (JASCO Co.: PU-980 Intelligent HPLC Pump, AS-950–10 Intelligent Sampler, CO-1560 Intelligent Column Thermostat, MD-1515 Multiwavelength Detector, Tokyo, Japan). Two milliliters of sample was injected directly onto a reversed phase C18 column (ULTRASPHERE ODS, 4.6 × 250 mm, 5 μm, Beckman Coulter, Inc.,) maintained at 40 °C. Solvent A was 0.01% formic acid, and solvent B was 0.01% formic acid-containing methanol. The column was equilibrated with a mixture of solvent A/solvent B (98/2, v/v). The compounds were eluted at a flow rate of 1.0 mL/min. A linear gradient was applied from 2 to 10% methanol over 20 min, kept at 10% for 5 min, lowered to 2% over 2 min, and equilibrated at these initial conditions for 15 min. The wavelength of the UV detector was set at 260 nm for the detection of dG and dA.

RESULTS

Optimal Condition for LC-MS/MS Detection. Figure 1 shows the product ion spectra for Luc-N^2-dG and N^6-dA adducts.

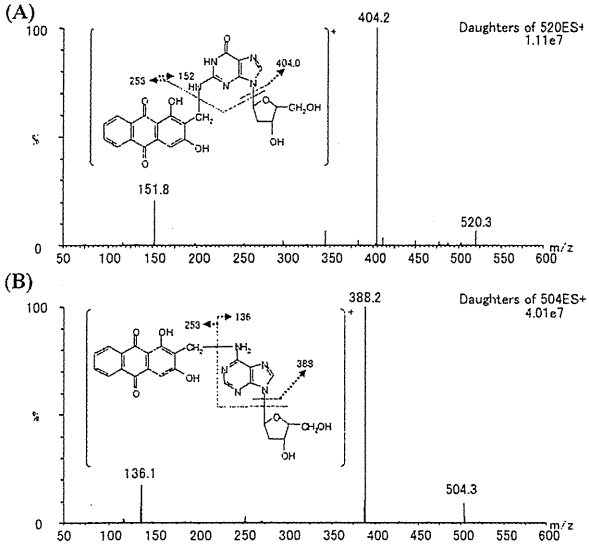

Figure 1. Product ion spectra of Luc-N^2-dG (A) and N^6-dA adducts (B). The cone voltages and collision energies were set at the optimal conditions for each compound in positive ion mode. LC-ESI-MS/MS conditions are described in Materials and Methods.

Positively ionized 2′-deoxynucleoside adducts and neutral loss of 2′-deoxyribose transmitting the $[M + H]^+ > [M + H\text{-}116]^+$ transition were observed. Although the combination of $[M + H]^+$ and $[M + H\text{-}116]^+$ as a precursor and daughter ion gave efficient ionization in both adducts, impurity peaks overlapped the Luc-N^2-dG adduct in MRM chromatograms of m/z 520 > 404 (Figure 2A). Therefore, m/z 152, which is the mass of guanosine, was selected as a daughter ion for the detection of the Luc-N^2-dG adduct. The mass spectrometer was equipped with an ESI source using a crossflow counter electrode and was run in the positive ion mode (ESI^+) and was used for MRM of the transitions 520 > 152 and 504 > 388. The MRM chromatograms obtained as a result of the addition of 0.01 nM standard and ^{15}N-labeled standard solutions to the control liver DNA sample are shown in Figure 2B–E. The crucial parameters affecting LC-ESI/MS/MS, namely, cone voltage, collision energy, and mobile phase, were investigated. In order to establish the optimal cone voltage and collision energy for the detection of

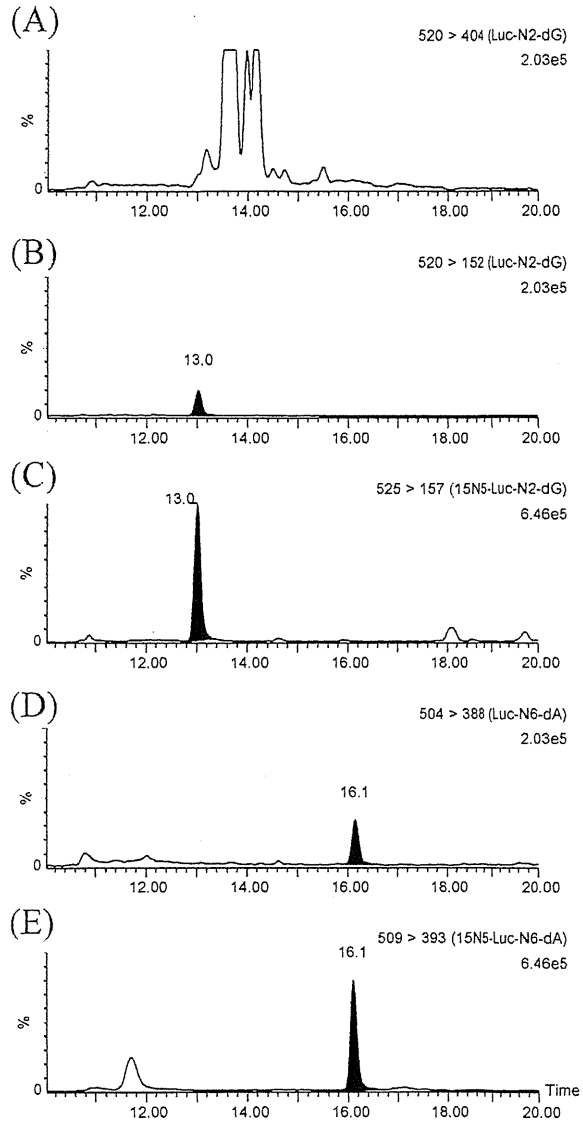

Figure 2. MRM chromatograms of the control liver DNA sample containing Luc-N^2-dG and N^6-dA standard and ^{15}N-labeled standard. The retention times of Luc-N^2-dG and N^6-dA were 13.0 and 16.0 min, respectively. Impurity peaks overlapped on the Luc-N^2-dG peak at m/z 520 > 404 (A). Luc-N^2-dG and ^{15}N-labeled standard peaks were detected at m/z 520 > 152 and 525 > 409 (B and C). Luc-N^6-dA and ^{15}N-labeled standard peaks were detected at m/z 504 > 388 and 509 > 393, respectively (D and E). Analytical conditions are described in Materials and Methods.

these adducts, m/z signals of 520 and 504 precursor ions versus cone voltage were investigated, respectively. The optimal cone voltages were 14 and 12 V in the positive ion mode for standard solutions of Luc-N^2-dG and N^6-dA adducts, respectively. Then, the signals of m/z 152 and 388 product ions versus collision energy were investigated. The optimal collision energies were 14 and 18 eV for standard solutions of Luc-N^2-dG and N^6-dA adducts, respectively. The ionization of the samples at the LC-MS interface is affected by the mobile phase; hence, a mobile phase containing a volatile acid or salt is frequently used. In this study, the responses were measured using 0–0.1% formic acid in

dx.doi.org/10.1021/tx300084p | Chem. Res. Toxicol. 2012, 25, 1112–1118

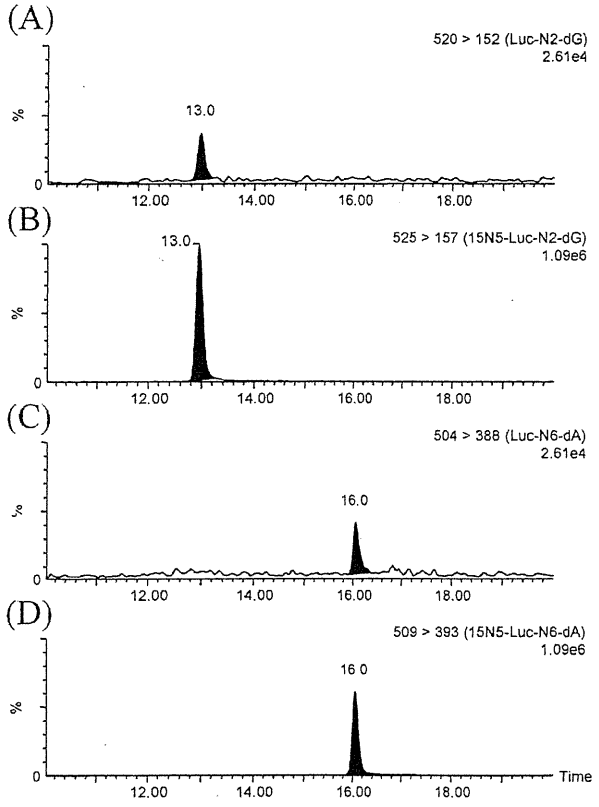

Figure 3. MRM chromatograms of Luc-N^2-dG and N^6-dA standards and their corresponding ^{15}N-labeled standards in 50% methanol at LOQ levels. (A) 0.5 nM Luc-N^2-dG, (B) $^{15}N_5$-Luc-N^2-dG, (C) Luc-N^6-dA and (D) $^{15}N_5$-Luc-N^6-dA. Analytical conditions are described in Materials and Methods.

Table 1. Recoveries of Luc-N^2-dG and N^2-dA Adducts from Control Rat Liver DNA Samples

compds	added[a] (pmol/L)	recovery (%)	RSD[b] (%)
Luc-N^2-dG (n = 5)	10	101.7 ± 6.2	6.1
	50	103.2 ± 8.3	8.0
	500	106.3 ± 2.5	2.3
Luc-N^6-dA (n = 5)	2	106.1 ± 4.0	3.8
	10	105.7 ± 6.1	5.8
	100	102.9 ± 3.0	2.9

[a]20 mM sodium acetate buffer (pH 4.2) with standard and adequate amount of ^{15}N-labeled standards was added to the DNA sample extracted from the livers of nontreated rats. After DNA digestion, Luc-N^2-dG andLuc-N^6-dA adducts were determined from five different samples in each concentration. [b]RSD: relative standard deviation.

water–acetonitrile (v/v) as the mobile phase. The responses of Luc-N^2-dG and N^6-dA adducts were increased by the addition of formic acid to the mobile phase. The increase in response reached a maximum and leveled off when 0.001% formic acid was added.

Validation of LC-MS/MS Analysis. The instrument quantification limits (IQL; S/N = 10) of Luc-N^2-dG and N^6-dA were 5 and 2.0 pM, respectively. The limits of detection (LOD) of Luc-N^2-dG and N^6-dA adducts in the DNA samples were 4.0 and 0.6 pM, and limits of quantification (LOQ) were 10 and 2.0 pM, respectively. The peak area ratio with respect to

Table 2. Interday Precision for the Determination of Luc-N^2-dG and N^2-dA Adducts Levels in the Liver of Rats Treated with 0.3% LuP for a Week on Four Different Days Using LC-MS/MS

	repeat analysis of Luc-N^2-dG adduct (nM)					
sample[a] no.	day 1[b]	day 2	day 3	day 4	mean (nmol/l)	RSD (%)[c]
1	151.1	147.1	141.6	145.9	145.9 ± 4.1	2.88
2	325.7	339.9	308.2	355.8	332.4 ± 20.8	6.10
3	292.6	283.8	262.0	296.7	283.8 ± 15.5	5.46
	repeat analysis of Luc-N^6-dA adduct (nM)					
sample[a] no.	day 1	day 2	day 3	day 4	mean (nmol/l)	RSD (%)
1	12.9	12.3	14.0	11.7	12.7 ± 1.0	7.78
2	21.8	22.4	20.6	20.2	21.3 ± 1.0	4.88
3	19.2	17.7	16.3	17.9	17.8 ± 1.2	6.67

[a]Livers of three different LuP-treated rats were used for interday precision for the determination of Luc-N^2-dG and N^6-dA adducts. [b]Analyses performed on four different days. [c]RSD: relative standard deviation.

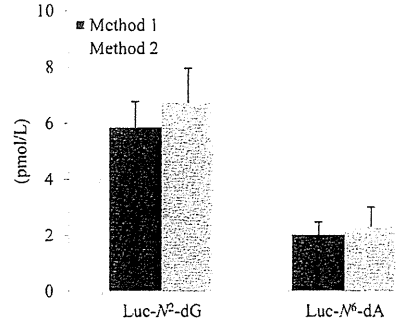

Figure 4. Luc-N^2-dG and N^6-dA levels in the livers of rats treated with 0.6% LuP following different digestion strategies. Each bar represents the mean ± SE for five animals. DNA digestion conditions are described in Materials and Methods.

each ^{15}N-labeled standard was plotted, and the response was found to be linear over the calibration range, from LOQ to 0.5 and 0.3 nM for Luc-N^2-dG and N^6-dA adducts, with a correlation coefficient (r) of over 0.999. The average retention times of Luc-N^2-dG and Luc-N^6-dA standards were 13.0 (relative standard deviation; RSD = 0.46%, n = 10) and 16.0 min (RSD = 0.31%, n = 10), respectively. MRM chromatograms of standard and their corresponding ^{15}N-labeled standard in 50% methanol at LOQ levels are shown in Figure 3. As shown in Table 1, the average recoveries of Luc-N^2-dG and N^6-dA adducts from DNA in the livers of nontreated rats ranged from 101.7 to 106.3 and 102.9 to 106.1%, respectively. Table 2 shows the interday precision for the detection of Luc-specific DNA adducts in the livers of rats treated with 0.3% LuP for a week. Analysis on four different days for interday precision using liver samples of three LuP-treated rats resulted in average RSD for Luc-N^2-dG and N^6-dA of 4.5 and 6.4%, respectively (Table 2).

Optimal Conditions for DNA Digestion. As shown in Figure 4, we did not observe significant differences between tests 1 and 2 in the levels of Luc-N^2-dG and N^6-dA adducts in the livers of rat treated with LuP. Since the overlapping noise peak of Luc-N^2-dG was detected in the chromatogram of all liver samples digested using method 2, method 1 was applied to

dx.doi.org/10.1021/tx300084p | Chem. Res. Toxicol. 2012, 25, 1112–1118

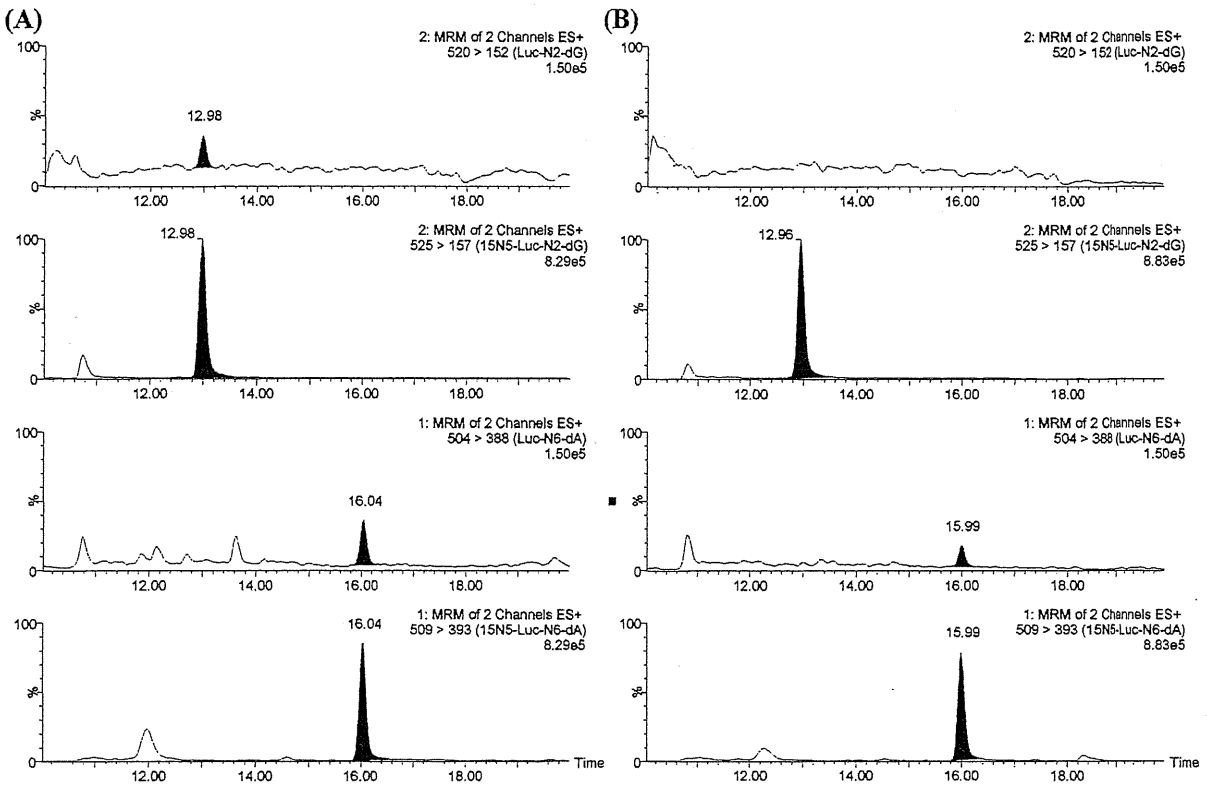

Figure 5. Typical MRM chromatograms of Luc-N^2-dG and N^6-dA adducts in the kidneys (A) and livers (B) of rats treated with 0.06% LuP. DNA digestion and analytical conditions are described in Materials and Methods.

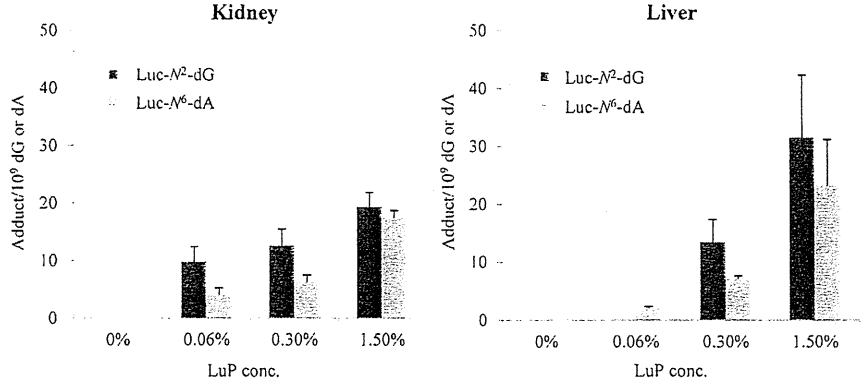

Figure 6. Luc-N^2-dG and N^6-dA levels in the kidneys and livers of rats treated with 0.06, 0.3, and 1.5% LuP. Each bar represents the mean ± SE for five animals. DNA digestion and analytical conditions are described in Materials and Methods.

the kidney and liver sample preparation as an optimal condition for DNA digestion.

Analysis of Luc-N^2-dG and N^6-dA Adducts in the Kidney and Liver DNA Isolated from Rats Treated with LuP. The potential formation of Luc-specific adducts in the livers and kidneys of rats exposed to LuP was assessed using the isotope dilution LC-ESI-MS/MS method. Both Luc-N^2-dG and N^6-dA adducts were detected at 13.0 and 16.0 min in the DNA MRM chromatograms extracted from kidneys of rats in the low dose group (Figure 5A), and adducts increased in a dose-dependent manner. Although Luc-N^2-dG was not detected in the livers of the low dose group (Figure 5B), dose-dependent increases of Luc-N^6-dA were observed. Quantitative data obtained from the kidney and liver DNAs are summarized in Figure 6. The amount of Luc-N^2-dG and N^6-dA was calculated as adducts/10^9dG and dA, respectively. Luc-N^2-dG and N^6-dA adducts were detected at ranges from 7.97 to 51.67 and 1.83 to 37.10/10^9 dG or dA, respectively, in the kidneys and livers of LuP-treated rats.

DISCUSSION

The existence of LuP- and Luc-related DNA adducts in the kidneys, livers, and duodenums of mice were previously shown by Poginsky et al. using ^{32}P-postlabeling analysis.[24] In our previous study, chemical structures of Luc-induced DNA

dx.doi.org/10.1021/tx300084p | Chem. Res. Toxicol. 2012, 25, 1112–1118

modification in the *in vitro* reaction were clarified to be Luc-N^2-dG and N^6-dA adducts by NMR analysis. In addition, the actual formation of these adducts in calf thymus DNA reacted with Luc in the presence of a S9 mixture was confirmed by LC-MS analysis.[7] However, it has remained uncertain whether the formation of these adducts actually occurred *in vivo* due to the low sensitivity of the analytical methods used. In the present study, an online sample purification method using column switching and an isotope dilution LC-ESI/tandem MS method using SIR to achieve higher sensitivities were developed for use with *in vivo* samples. The advantage of the online column-switching system is that an enzymatically hydrolyzed DNA sample can be analyzed directly without removing excess unmodified 2-deoxynucleosides believed to interfere with the analysis.[25,26] We have applied a similar approach for the determination of DNA adducts derived from reactive nitrogen species and also demonstrated that the column-switching system is useful for DNA sample analysis.[27] Addition of ^{15}N-labeled internal standards prior to enzymatic hydrolysis of the DNA samples allows for the accurate quantification of DNA adducts and also provides confirmation of the identity of the analyte peak since it elutes at a retention time identical to that of the unlabeled analyte. Given these advantages, our method permitted highly sensitive detection of Luc-N^2-dG and N^6-dA adducts at levels of 2–10 adducts/10^9 dG or dA as LOQ levels, which was 100-times higher in sensitivity than the previous LC-MS method.[7] In addition, the high recoveries of these adducts in the wide range of LOQ levels indicated that our new method enables the precise determination of adducts with the use of their ^{15}N-labeled standard and is applicable to the detection of these adducts in *in vivo* samples.

Following DNA isolation, enzymatic digestion of DNA greatly influences the ability of the detection methods to identify DNA adducts. Since our detection methods identify adducted nucleosides produced by the hydrolysis of duplex DNA, incomplete hydrolysis results in the formation of oligonucleotides which are incorrectly identified as other adducts by mass spectrometry. Therefore, the hydrolysis of DNA to yield a mixture of natural and adducted nucleosides was optimized to provide structural information about specific DNA adducts. Quantitative data obtained from the digestion of Luc-N^2-dG and N^6-dA adducts using two strategies showed that there were no differences in digestion efficiencies between nuclease P1/alkaline phosphatase with and without VPDE/SPDE. In addition, VPED/SPDE resulted in a noise peak on the MRM chromatograms in spite of the passage of the samples through a membrane filter (data not shown). These results led us to conclude that nuclease P1/alkaline phosphatase is a suitable method for Luc-N^2-dG and N^6-dA adducts analysis.

To confirm the availability of this analytical method for use *in vivo*, the levels of Luc-N^2-dG and N^6-dA adducts were measured in liver and kidney DNAs of rats treated for one week with LuP at concentrations of 0.06, 0.3, and 1.5% in the diet. Our method was able to quantify two adducts, in kidney and liver DNAs of LuP-treated rats, and we showed that there were no differences in the amounts of DNA adducts between the two organs.

MC, including LuP, is a potent carcinogen, targeting the kidneys and livers of F344 rats. The incidence in the kidney is higher than that in liver.[2] However, there were no correlation between the amount of DNA damage in the organ and carcinogenic potential at the site. Our recent study clearly showed that ochratoxin A is capable of inducing a site-specific deletion mutation in the outer medulla of rat kidneys in spite of a lack of *in vivo* mutagenicity in total kidney DNA.[28] In addition to the fact that MC-induced renal tumors were found in the outer medulla, we reported that metabolites of LuP also induce site-specific renal toxicity, such as karyomegaly and atypical hyperplasia of proximal tubules in the outer medulla.[29,30] These site-specific changes may be due to MC or LuP localization in the kidneys, which might explain the lack of differences in the amounts of DNA adducts between total kidney and liver DNA. As another explanation, interorgan differences of carcinogenic susceptibility may be considered.[31] Although further examinations are necessary to clarify the association between DNA adduct formation and carcinogenic susceptibility, the overall data allow us to conclude that the formation of Luc-specific DNA adducts may be an important key to MC carcinogenesis.

In conclusion, our newly developed technique involves online sample purification methodology using column-switching and an isotope dilution LC-ESI/tandem MS method using SIR. It is capable of achieving sufficient analytical sensitivities for use with *in vivo* samples. As a result, the formation of Luc-specific adducts following exposure to MC or LuP was confirmed. This new methodology may help us to understand MC-induced carcinogenesis.

AUTHOR INFORMATION

Corresponding Author

*Tel: +81-3-3700-9819. Fax: +81-3-3700-1425. E-mail: y-ishii@nihs.go.jp.

Notes

The authors declare no competing financial interest.

ABBREVIATIONS

LuP, lucidin-3-*O*-premeveroside; MC, madder color; Luc, lucidin; Rub, rubiadin; Alz, alizarin; CS, column switching; SIR, selected ion recording; LC, liquid chromatography; ESI, electron spray ionization; MS, mass spectrometry; MS/MS, tandem mass spectrometry; dG, 2′-deoxyguanosine; dA, 2′-deoxyadenosine; VPDE, phosphodiesterase I from *Crotalus adamanteus* venom; SPDE, phosphodiesterase II from bovine spleen; IQL, instrument quantification limit; LOD, limit of detection; LOQ, limit of quantification; RSD, relative standard deviation

REFERENCES

(1) MHLW (Ministry of Health, Labor and Welfare of Japan) (1995) List of Existing Food Additives (in Japanese), in *Foods and Food Ingredients (Editorial)*, Vol. *166*, pp 93–101.

(2) Inoue, K., Yoshida, M., Takahashi, M., Shibutani, M., Takagi, H., Hirose, M., and Nishikawa, A. (2009) Induction of kidney and liver cancers by the natural food additive madder color in a two-year rat carcinogenicity study. *Food Chem. Toxicol. 47*, 184–191.

(3) Blömeke, B., Poginsky, B., Schmutte, C., Marquardt, H., and Westendorf, J. (1992) Formation of genotoxic metabolites from anthraquinone glycosides, present in *Rubia tinctrum* L. *Mutat. Res. 265*, 263–272.

(4) Brown, J. P., and Dietrich, P. S. (1979) Mutagenicity of anthraquinone and bezanthrone derivatives in the Salmonella/microsome test: activation of anthraquinone glycoside enzymic extracts of rat cecal bacteria. *Mutat. Res. 66*, 9–24.

(5) Kawasaki, Y., Goda, Y., and Yoshihira, K. (1992) The mutagenic constituents of *Rubia tinctorum*. *Chem. Pharm. Bull. 40*, 1504–1509.

(6) Yasui, Y., and Takeda, N. (1983) Identification of mutagenic substance, in *Rubia tinctorum* L. (madder) root, as lucidin. *Mutat. Res. 121*, 185–190.

(7) Ishii, Y., Okamura, T., Inoue, T., Fukuhara, K., Umemura, T., and Nishikawa, A. (2010) Chemical structure determination of DNA bases

modified by active metabolites of lucidin-O-primeveroside. *Chem. Res. Toxicol. 23*, 134−141.

(8) Kim, H. Y., Cooper, M., Nechev, L. V., Harris, C. M., and Harris, T. M. (2001) Synthesis and characterization of nucleosides and oligonucleotides with benzo[a]pyren-6-ylmethyl adduct at adenine N6 or guanine N2. *Chem. Res. Toxicol. 14*, 1306−1314.

(9) Arlt, V. M., Schmeiser, H. H., Osborne, M. R., Kawanishi, M., Kanno, T., Yagi, T., Phillips, D. H., and Takamura-Enya, T. (2006) Identification of three major DNA adducts formed by the carcinogenic air pollutant 3-nitrobenzanthrone in rat lung at the C8 and N2 position of guanine at the N6 position of adenine. *Int. J. Cancer 118*, 2139−2146.

(10) Rodriguez, H., and Loechler, E. L. (1993) Mutational spectra of the (+)-anti-diol epoxide of benzo[a]pyrene in supF gene of an Escherichia coli plasmid: DNA sequence context influences hotspots, mutational specificity and the extent of SOS enhancement of mutagenesis. *Carcinogenesis 14*, 373−383.

(11) Rodriguez, H., and Loechler, E. L. (1993) Mutagenesis by the (+)-anti-diol epoxide of benzo[a]pyrene: what controls mutagenic specificity? *Biochemistry 32*, 373−383.

(12) Seo, K. Y., Nagalingam, A., Tiffany, M., and Loechler, E. L. (2005) Mutagenesis studies with four stereoisomeric N2-dG benzo-[a]pyrene adducts in the identical 5′-CGC sequence used in NMR studies: G > T mutations dominate in each case. *Mutagenesis 20*, 441−448.

(13) Zhao, B., Wang, J., Geacintow, N. E., and Wang, Z. (2006) Poleta, Polzeta and Rev1 together are required for G to T transversion mutations induced by the (+)-and ,(-)-trans-anti-BPDE-N2-dG DNA adducts in yeast cells. *Chem. Res. Toxicol. 34*, 417−425.

(14) Nagy, E., Zeising, M., Kawamura, K., Hisamatsu, Y., Sugeta, A., Adachi, S., and Möller, L. (2005) DNA adduct and tumor formations in rats after intratracheal administration of the urban air pollutant 3-nitrobenzabthrone. *Carcinogenesis 26*, 1821−1828.

(15) Arlt, V. M. (2005) 3-Nitrobenzanthrone, a potential human cancer hazard in diesel exhaust and urban air pollution: a review of the evidence. *Mutagenesis 20*, 399−410.

(16) Zhang, Y., Wu, X., Guo, D., Rechkoblit, O., and Wang, Z. (2002) Activities of human DNA polymerase kappa in response to the major benzo[a]pyrene DNA adduct: error-free lesion bypass and extension synthesis from opposite the lesion. *DNA Repair 1*, 559−569.

(17) Moustacchi, E. (2000) DNA damage and repair: consequences on dose-responses. *Mutat. Res. 464*, 35−40.

(18) Prakash, A. S., Tran, H. P., Peng, C., Koyalamudi, S. R., and Dameron, C. T. (2000) Kinetics of DNA alkylation, depurination and hydrolysis of anti diol epoxide of benzo(a)pyrene and the effect of cadmium on DNA alkylation. *Chem.-Biol. Interact 125*, 133−150.

(19) Singh, R., Gaskell, M., Le Pla, R. C., Kaur, B., Azim-Araghi, A., Roach, J., Koukouves, G., Souliotis, V. L., Kyrtopoulos, S. A., and Farmer, P. B. (2006) Detection and quantitation of benzo[a]pyrene-derived DNA adducts in mouse liver by liquid chromatography-tandem mass spectrometry: comparison with ^{32}P-postlabeling. *Chem. Res. Toxicol. 19*, 868−878.

(20) Ishii, Y., Suzuki, Y., Hibi, D., Jin, M., Fukuhara, K., Umemura, T., and Nishikawa, A. (2011) Detection and quantitation of specific DNA adducts by liquid chromatography-tandem mass spectrometry in the livers of rats given estragole at the carcinogenic dose. *Chem. Res. Toxicol. 24*, 532−541.

(21) Wang, M., Lao, Y., Cheng, G., Shi, Y., Villalta, P. W., Nishikawa, A., and Hecht, S. S. (2007) Analysis of adducts in hepatic DNA of rats treated with N-nitrosopyrrolidine. *Chem. Res. Toxicol. 20*, 634−640.

(22) Koc, H., and Swenberg, J. A. (2002) Application of mass spectrometry for quantitation of DNA adducts. *J. Chromatogr., B 778*, 323−33.

(23) Delatour, T., Mally, A., Richoz, J., Ozden, S., Dekant, W., Ihmels, H., Otto, D., Gasparutto, D., Marin-Kuan, M., Schilter, B., and Cavin, C. (2008) Absence of 2′-deoxyguanosine-carbon 8-bound ochratoxicn A adduct in rat kidney DNA monitored by isotope dilution LC-MS/MS. *Mol. Nutr. Food. Res. 52*, 472−482.

(24) Poginsky, B., Westendorf, J., Blömeke, B., Marquardt, H., Hewer, A., Grover, P. L., and Phillips, D. H. (1991) Evaluation of DNA-binding activity of hydrosyanthraquinones occurring in *Rubia tinctorum* L. *Carcinogenesis 12*, 1265−1271.

(25) Singh, R., Arlt, V. M., Henderson, C. J., Phillips, D. H., Farmer, P. B., and Gamboa da Costa, G. (2010) Detection and quantitation of N-(deoxyguanosine-8-yl)-2-amino-1-methyl-6-phenylimidazo[4,5-b]-pyridine adducts in DNA using online column-switching liquid chromatography tandem mass spectrometry. *J. Chromatogr., B 878*, 2155−2162.

(26) Gamboa da Costa, G., Singh, R., Arlt, V. M., Mirza, A., Richards, M., Takamura-Enya, T., Schmeiser, H. H., Farmer, P. B., and Phillips, D. H. (2009) Quantification of 3-nitrobenzanthorone-DNA adducts using online column-switching HPLC-electrospray tandem mass spectrometry. *Chem. Res. Toxicol. 22*, 1860−1868.

(27) Ishii, Y., Ogara, A., Okamura, T., Umemura, T., Nishikawa, A., Iwasaki, Y., Ito, R., Saito, K., Hirose, M., and Nakazawa, H. (2007) Development of quantitative analysis of 8-nitroguanine concomitant with 8-hydroxydeoxyguanosine formation by liquid chromatography with mass spectrometry and glyoxal derivatization. *J. Pharm. Biomed. Anal. 43*, 1737−1743.

(28) Hibi, D., Suzuki, Y., Ishii, Y., Jin, M., Watanabe, M., Sugita-Konishi, Y., Yanai, T., Nohmi, T., Nishikawa, A., and Umemura, T. (2011) Site-specific in vivo mutagenicity in the kidney of gpt delta rats given a carcinogenic dose of ochratoxin A. *Toxicol. Sci. 122*, 406−414.

(29) Inoue, K., Yoshida, M., Takahashi, M., Fujimoto, H., Shibutani, M., Hirose, M., and Nishikawa, A. (2009) Carcinogenic potential of alizarin and rubiadin, components of madder color, in a rat medium-term multi-organ bioassay. *Cancer Sci. 100*, 2261−2267.

(30) Inoue, K., Yoshida, M., Takahashi, M., Fujimoto, H., Ohnishi, K., Nakashima, K., Shibutani, M., Hirose, M., and Nishikawa, A. (2009) Possible contribution of rubiadin, a metabolite of madder color, to renal carcinogenesis in rats. *Food Chem. Toxicol. 47*, 752−759.

(31) Bedard, L. L., Alessi, M., Davey, S., and Massey, T. E. (2005) Susceptibility to afratoxin B1-induced carcinogenesis correlates with tissue-specific differences in DNA repair activity in mouse and in rat. *Cancer Res. 65*, 1265−1270.

Toxicology 290 (2011) 312–321

Contents lists available at SciVerse ScienceDirect

Toxicology

journal homepage: www.elsevier.com/locate/toxicol

Comprehensive toxicity study of safrole using a medium-term animal model with *gpt* delta rats

M. Jin[a], A. Kijima[a], Y. Suzuki[a], D. Hibi[a], T. Inoue[a], Y. Ishii[a], T. Nohmi[b], A. Nishikawa[c], K. Ogawa[a], T. Umemura[a,*]

[a] Division of Pathology, National Institute of Health Sciences, 1-18-1 Kamiyoga, Setagaya-ku, Tokyo 158-8501, Japan
[b] Sciences of Genome Safety, National Institute of Health Sciences, 1-18-1 Kamiyoga, Setagaya-ku, Tokyo 158-8501, Japan
[c] Biological Safety Research Center, National Institute of Health Sciences, 1-18-1 Kamiyoga, Setagaya-ku, Tokyo 158-8501, Japan

ARTICLE INFO

Article history:
Received 8 September 2011
Received in revised form
29 September 2011
Accepted 30 September 2011
Available online 15 October 2011

Keywords:
Medium-term animal model
gpt delta
In vivo genotoxicity
Safrole

ABSTRACT

In order to investigate a medium-term animal model using reporter gene transgenic rodents in which general toxicity, genotoxicity and carcinogenicity are evaluated, F344 *gpt* delta rats were given a diet containing 0.1% and 0.5% (a carcinogenic dose) safrole for 13 weeks. Serum biochemistry and histopathological examinations revealed overt hepatotoxicity of safrole, in line with previous reports. In the current study, safrole treatment possibly resulted in renal toxicity in male rats. In the *in vivo* mutation assays, an increase or a tendency to increase of the *gpt* mutant frequencies (MFs) was observed in both sexes at the carcinogenic dose. The number and area of foci of glutathione S-transferase placental form (GST-P) positive hepatocytes, ratio of proliferating cell nuclear antigen (PCNA)-positive hepatocytes and 8-hydroxydeoxyguanosine (8-OHdG) levels in liver DNA were significantly increased in both sexes of the 0.5% group. The overall data suggested that the present model might be a promising candidate for investigating comprehensive toxicities of the agents. In addition, data demonstrating the base modification and cell proliferation due to exposure to safrole could contribute to understanding safrole-induced hepatocarcinogenesis, which imply expanding in application of this model.

1. Introduction

According to Environmental Health Criteria; 240 (EHC240) by the Joint FAO/WHO Expert Committee on Food Additives (JECFA), the safety assessment of food additive should be evaluated based on data such as various genotoxicity, repeated dose toxicity and carcinogenicity tests. However, these studies are time-intensive and require the extensive use of laboratory animals. Thus, the development of a new medium-term animal model in which general toxicity, genotoxicity and carcinogenicity in target organs can be collectively evaluated is desired in terms of the 3R's (Reduction of experimental animals, Refinement of pain of experimental animal and Replacement of animal experiments) of animal testing.

The *gpt* delta rat is one of the reporter gene transgenic rats and carries approximately five tandem copies of the transgene lambda EG10 per haploid genome. It is well recognized that an *in vivo* mutation assay using *gpt* delta rats can detect not only point mutations by 6-TG selection, but also deletion mutations by Spi$^-$ selection (Hayashi et al., 2003; Umemura et al., 2009; Masumura et al., 2003). In addition, the glutathione S-transferase placental (GST-P) from positive preneoplastic hepatic foci can be analyzed in the *gpt* delta rats (Toyoda-Hokaiwado et al., 2010). Accordingly, the use of *gpt* delta rats enables us to examine 90-day repeated dose toxicity, *in vivo* genotoxicity and carcinogenicity tests as analysis of preneoplastic changes in a single study.

Safrole (4-allyl-1,2-methylenedioxybenzene) is a natural plant constituent found in the essential oils of sassafras, sweet basil, cinnamon and spices (Furia and Bellanca, 1975; Leung, 1980; Ioannides et al., 1981). Safrole is a hepatocarcinogen in mice and rats fed as 0.5–1% of the diet of mice and rats (Borchert et al., 1973; IARC, 1976; Wislocki et al., 1977). In addition, exposure of safrole resulted in liver toxicity in short-term studies using rats (Hagan et al., 1965). It was reported that safrole-specific DNA adducts were formed following the hepatic cytochrome P450 biotransformation of safrole to 1′-hydroxy-safrole (Daimon et al., 1998) and that high doses of safrole induced oxidative DNA damage in the livers of Sprague Dawley rats (Liu et al., 1999). However, safrole was not mutagenic in *Salmonella typhimurium* TA98 (Dorange et al., 1978; To et al., 1982). In other studies, conventional genotoxicity tests such as the Ames test, sister chromatid exchange (SCE) test and micronucleus test were positive (Natarajan and Darroudi, 1991). Accordingly, it is unclear whether safrole has an *in vivo* genotoxicity, and genotoxic mechanisms are involved in its hepatocarcinogenesis.

* Corresponding author. Tel.: +81 03 3700 9819; fax: +81 03 3700 1425.
E-mail address: umemura@nihs.go.jp (T. Umemura).

0300-483X/$ – see front matter © 2011 Elsevier Ireland Ltd. All rights reserved.
doi:10.1016/j.tox.2011.09.088

Table 1
Final body weight and diet consumptions and test substance intake in F344 *gpt* delta rats given diet containing safrole for 13 weeks.

Sex	Groups	No. of animals	Final body weight (g)	Diet consumption (g/rat/day)	Daily intake of test substance (mg/kg/day)
Male	Control	10	369.5 ± 24.5[a]	18.0 ± 2.0	0.0 ± 0.0
	0.1% safrole	10	341.1 ± 20.0**	16.2 ± 1.8	60.6 ± 13.4
	0.5% safrole	10	264.4 ± 13.0**	12.6 ± 2.4	274.5 ± 61.9
Female	Control	9	202.1 ± 7.8	12.7 ± 1.6	0.0 ± 0.0
	0.1% safrole	10	168.7 ± 10.3**	10.0 ± 0.9	69.1 ± 13.9
	0.5% safrole	10	150.1 ± 8.6**	7.4 ± 1.7	275.6 ± 77.9

[a] Mean ± SD.
** Significantly different from the control group at the levels of $p < 0.01$ (Dunnett's test).

In the present study, to confirm availability of a medium-term animal model using *gpt* delta rats, we examined repeated dose toxicity, *in vivo* genotoxicity and possible carcinogenicity in *gpt* delta rats given safrole at two doses, including a carcinogenic dose, for 13 weeks together with measurements of oxidative DNA damage and cell proliferation in the liver.

2. Materials and methods

2.1. Chemicals

Safrole and corn oil were purchased from Tokyo Kasei (Tokyo, Japan) and Wako Pure Chemical Industries (Osaka, Japan), respectively. Alkaline phosphatase was obtained from Sigma Chemical (St. Louis, MO, USA) and nuclease P1 was from Yamasa Shoyu (Chiba, Japan).

2.2. Animals, diet and housing conditions

The protocol for this study was approved by the Animal Care and Utilization Committee of the National Institute of Health Sciences (Tokyo, Japan). Five-week-old male and female F344 *gpt* delta rats carrying approximately five tandem copies of the transgene lambda EG10 per haploid genome were obtained from Japan SLC (Shizuoka, Japan). They were housed in polycarbonate cages (three or four rats per cage) with hardwood chips for bedding in a conventional animal facility. Animals were maintained under conditions of controlled temperature (23 ± 2 °C), humidity (55 ± 5 °C), air change (12 times per hour), and lighting (12 h light/dark cycle).

Table 2
Hematological data for F344 *gpt* delta rats given diet containing safrole for 13 weeks.

	Groups		
	Control	0.1% safrole	0.5% safrole
Males			
No. of animals examined	10	10	10
WBC (×10²/μl)	54.1 ± 5.5[a]	46.1 ± 7.7*	46.5 ± 5.8*
RBC (×10⁴/μl)	976.7 ± 37.3	964.1 ± 42.1	919.1 ± 33.9**
Hb (g/dl)	15.6 ± 0.2	15.6 ± 0.2	15.4 ± 0.5
Ht (%)	51.1 ± 2.1	51.1 ± 2.1	50.0 ± 1.8
MCV (fl)	52.2 ± 0.4	53.0 ± 0.4**	54.3 ± 0.3**
MCH (pg)	16.2 ± 0.6	16.2 ± 0.6	16.7 ± 0.4**
MCHC (g/dl)	30.5 ± 1.0	30.5 ± 1.0	30.8 ± 0.7
Plt (×10⁴/μl)	72.8 ± 4.2	66.1 ± 4.2**	71.6 ± 5.7
Differential leukocyte counts (%)			
Band form neutrophils	1.4 ± 0.9	2.3 ± 2.0	1.7 ± 0.6
Segmented neutrophils	36.7 ± 7.8	31.9 ± 4.9	37.6 ± 6.6
Eosinophils	1.9 ± 0.9	1.1 ± 0.9	1.4 ± 1.2
Basophils	0.0 ± 0.0	0.0 ± 0.0	0.0 ± 0.0
Lymphocytes	59.5 ± 8.2	61.0 ± 13.8	59.2 ± 7.0
Monocytes	0.6 ± 0.4	0.3 ± 0.3	0.1 ± 0.2**
Reticulocytes	1.8 ± 1.6	0.4 ± 0.9	0.6 ± 1.3
Females			
No. of animals examined	9	10	10
WBC (×10²/μl)	34.9 ± 5.6	34.6 ± 10.6	44.8 ± 8.9*
RBC (×10⁴/μl)	923.5 ± 31.9	916.5 ± 31.0	896.7 ± 29.3
Hb (g/dl)	15.8 ± 0.6	15.5 ± 0.6	15.4 ± 0.4
Ht (%)	51.7 ± 2.0	50.9 ± 1.8	50.0 ± 1.6
MCV (fl)	56.0 ± 0.5	55.6 ± 0.4*	55.8 ± 0.4
MCH (pg)	17.2 ± 0.2	17.0 ± 0.2	17.2 ± 0.4
MCHC (g/dl)	30.6 ± 0.5	30.5 ± 0.3	30.8 ± 0.7
Plt (×10⁴/μl)	74.6 ± 8.1	72.4 ± 2.7	59.3 ± 3.3**
Differential leukocyte counts (%)			
Band form neutrophils	1.9 ± 1.1	1.0 ± 0.7	0.5 ± 0.4*
Segmented neutrophils	28.4 ± 6.0	22.2 ± 6.7	19.3 ± 47**
Eosinophils	1.6 ± 1.0	1.0 ± 0.4	0.7 ± 0.5*
Basophils	0.0 ± 0.0	0.0 ± 0.0	0.0 ± 0.0
Lymphocytes	68.0 ± 7.0	75.3 ± 7.0*	79.2 ± 4.6**
Monocytes	0.2 ± 0.3	0.5 ± 0.4	0.5 ± 0.3
Reticulocytes	5.4 ± 3.7	2.8 ± 2.8	1.0 ± 0.8**

Abbreviations: WBC, white blood cell; RBC, red blood cell; Hb, hemoglobin; Ht, hematocrit; MCV, mean corpuscular volume; MCH, mean corpuscular hemoglobin; MCHC, mean corpuscular hemoglobin concentration; PI, platelet.
[a] Mean ± SD.
* Significantly different from the controls at the levels of $p < 0.05$ (Dunnett's test).
** Significantly different from the controls at the levels of $p < 0.01$ (Dunnett's test).

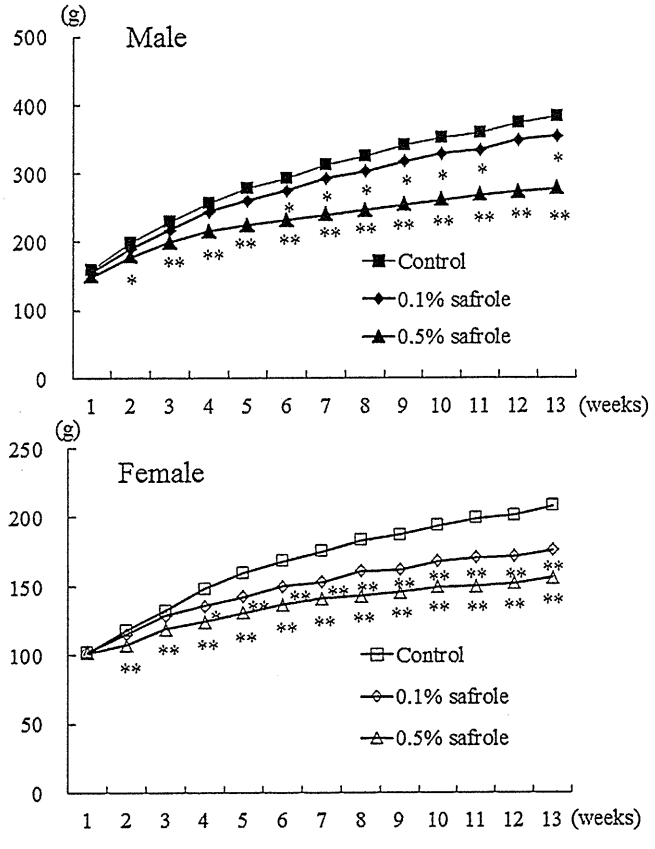

Fig. 1. Body weight curves for F344 *gpt* delta rats given safrole for 13 weeks. *,**: significantly different from the control group at $p < 0.05$ and $p < 0.01$, respectively.

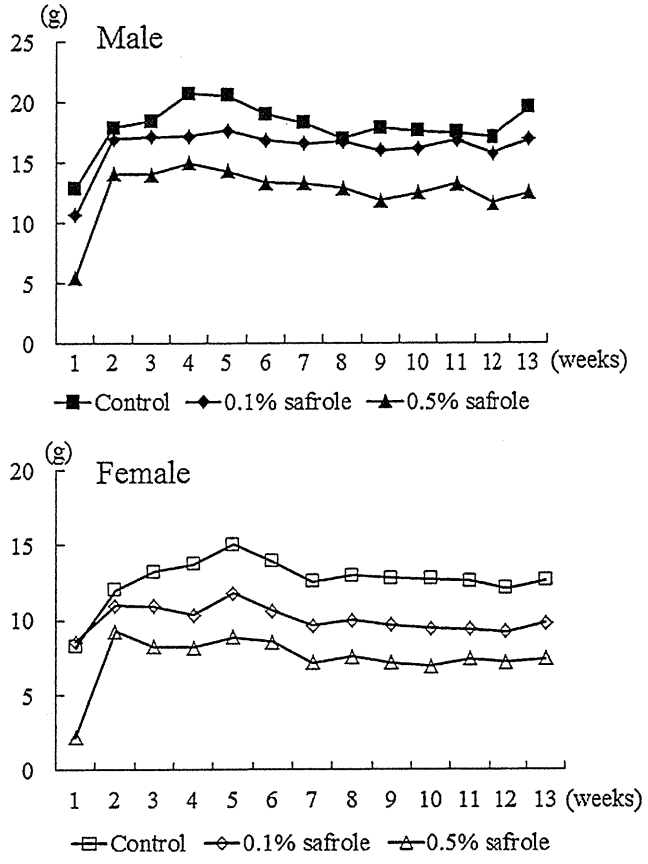

Fig. 2. Daily food intake for F344 *gpt* delta rats given safrole for 13 weeks. *,**: significantly different from the control group at $p < 0.05$ and $p < 0.01$, respectively.

Animals were given free access to a CRF-1 basal diet (Charles River Japan, Kanagawa, Japan) and tap water.

2.3. Experimental design

After a 1-week acclimatization period, animals were divided into 3 groups consisting of 10 male and 10 female F344 *gpt* delta rats per group, and given a diet containing 0.1%, 0.5% or 0% safrole for 13 weeks.

Clinical signs and general appearance were observed once a day. Body weight and food consumption were measured once a week. At the end of each period, the animals were euthanized under deep anesthesia. Left liver lobes were fixed with neutral-buffered formalin for histopathological and immunohistopathological examination. The remaining liver was stored at −80 °C for 8-OHdG measurements and *in vivo* mutation assays. At necropsy, blood samples were collected from the abdominal aorta for hematology and serum biochemistry. Relative organ weights were calculated as the values relative to body weights.

Hematological analysis was performed using an automated hematology analyzer, K-4500 (Sysmex Corp., Hyogo, Japan). Differential leukocyte and reticulocyte count were performed with a MICROX HEG-505 (Sysmex Corp.). Parameters for serum biochemistry shown in Table 3 were analyzed at SRL, Inc. (Tokyo, Japan) using sera frozen after centrifugation of whole blood.

At autopsy, weights of brain, heart, lungs, liver, kidneys, spleen, thymus, adrenal glands and testes were measured. In addition to these organs, the artery, bone/marrow, coagulation gland, esophagus, epididymides, large intestine (cecum, colon, and rectum), lymph node, mammary gland, pancreas, peripheral nerve, prostate gland, pituitary gland, thyroid glands, salivary gland, skeletal muscle, skin, small intestine (duodenum, jejunum, and ileum), spinal cord, stomach, urinary bladder, tongue, trachea, vagina, uterus, and ovaries were fixed in 10% neutral buffered formalin. Testes were fixed in Bouin's solution overnight and then transferred into 10% neutral buffered formalin. Tissues that needed decalcification, such as the nasal cavity, spinal cord with bones, sternum, and femur, were treated with a mixture of 10% formic acid and 10% neutral phosphate-buffered formalin. These tissues were routinely embedded in paraffin, sectioned at 3 μm thick for hematoxylin and eosin staining, and examined under light microscopy. Histopathological examinations were carried out for all groups.

2.4. In vivo mutation assays

The 6-TG and Spi⁻ (insensitive P2 interference) selection was carried out as previously described (Nohmi et al., 1996, 2000). Briefly, genomic DNA was extracted from liver tissue, and lambda EG10 DNA (48 kb) was rescued as the lambda phage through *in vitro* packaging. For 6-TG selection, the packaged phage was incubated with *E. coli* YG6020, expressing Cre recombinase, and converted to a plasmid carrying *gpt* and chloramphenicol acetyltransferase. Infected cells were mixed with molten soft agar and poured onto agar plates containing chloramphenicol and 6-TG. In order to determine the total number of rescued plasmids, infected cells were also poured on plates containing chloramphenicol without 6-TG. The plates were incubated at 37 °C for the selection of 6-TG resistant colonies, and the *gpt* mutant frequency (MF) was calculated by dividing the number of *gpt* mutants after clonal correction by the number of rescued phages. To characterize *gpt* mutations, a 739 bp DNA fragment containing the 456 bp coding region of the *gpt* gene was amplified by PCR as previously described, and the PCR products were analyzed with Applied Biosystems 3730 × 1 DNA Analyzer (Applied Biosystems Japan Ltd).

For Spi⁻ selection, the packaged phage was incubated with *E. coli* XL-1 Blue MRA for survival titration and *E. coli* XL-1 Blue MRA P2 for mutant selection. Infected cells were mixed with molten lambda-trypticase agar plates. The next day, plaques (Spi⁻ candidates) were punched out with sterilized glass pipettes and the agar plugs were suspended in SM buffer. In order to confirm the Spi⁻ phenotype of candidates, the suspensions were spotted on three types of plates containing XL-1 Blue MRA, XL-1 Blue MRA P2, or WL95 P2 strains and were spread with soft agar. The numbers of mutants that made clear plaques on each plate were counted as confirmed Spi⁻ mutants. The Spi⁻ MF was calculated by dividing the number of Spi⁻ mutants by the number of rescued phages. In all *in vivo* mutations assays, positive DNA samples were simultaneously applied to ensure the procedures well.

2.5. Measurement of nuclear 8-OHdG

In order to prevent 8-OHdG formation as a by-product during DNA isolation (Kasai, 2002), liver DNA was extracted using a slight modification of the method by Nakae et al. (1995). Briefly, nuclear DNA was extracted with a DNA Extractor WB Kit (Wako Pure Chemical Industries) containing an antioxidant NaI solution to dissolve cellular components. For further prevention of auto-oxidation in the cell lysis step, deferoxamine mesylate (Sigma Chemical, St. Louis, MO, USA) was added to the lysis buffer. The DNA was digested to deoxynucleotides by treatment with nuclease P1 and alkaline phosphatase and the levels of 8-OHdG (8-OHdG/10^5 dG) were measured by high-performance liquid chromatography with an electrochemical detection system (Coulochem II; ESA, Bedford, MA, USA).

Table 3
Serum biochemistry for F344 *gpt* delta rats given safrole for 13 weeks.

	Groups		
	Control	0.1% safrole	0.5% safrole
Males			
No. of animals examined	10	10	10
TP (g/dl)	7.0 ± 0.2[a]	7.0 ± 0.2	7.2 ± 0.2
A/G	2.0 ± 0.1	2.2 ± 0.1**	2.3 ± 0.1**
Alb (g/dl)	4.7 ± 0.1	4.8 ± 0.1	5.0 ± 0.2**
T-Bil (mg/dl)	0.04 ± 0	0.04 ± 0.01	0.03 ± 0.01**
Glucose (mg/dl)	159.3 ± 9.2	150.9 ± 7.2*	128.1 ± 3.9**
TG (mg/dl)	132.6 ± 61.8	83.3 ± 24.5	60.8 ± 23.7**
Phospholipid (mg/dl)	125.1 ± 16.7	117.4 ± 9.6	147.2 ± 12.5**
TC (mg/dl)	78.1 ± 6.5	76.3 ± 6.4	105.6 ± 9.8**
BUN (mg/dl)	19.3 ± 1.5	20.1 ± 0.7	23.6 ± 1.6**
CRN (mg/dl)	0.32 ± 0.01	0.34 ± 0.03	0.36 ± 0.03**
Na (mequiv./l)	145.9 ± 0.7	144.9 ± 0.7*	145.8 ± 1.1
Cl (mequiv./l)	106.1 ± 0.9	104.5 ± 1.2**	104.1 ± 1.3**
K (mequiv./l)	4.5 ± 0.2	4.4 ± 0.1	3.9 ± 0.9*
Ca (mg/dl)	10.8 ± 0.2	10.7 ± 0.2	11.2 ± 0.2**
IP (mg/dl)	5.7 ± 0.3	6.1 ± 0.5	6.0 ± 0.4
AST (IU/l)	98.9 ± 12.1	103.1 ± 7.0	117.4 ± 12.1**
ALT (IU/l)	54.1 ± 6.1	55.9 ± 4.8	102.7 ± 16.2**
ALP (IU/l)	497.3 ± 41.2	462.9 ± 49.1	375.0 ± 30.3**
Females			
No. of animals examined	9	10	10
TP (g/dl)	7.2 ± 0.3	6.6 ± 0.2**	6.9 ± 0.2*
A/G	2.7 ± 0.2	2.7 ± 0.1	2.6 ± 0.1
Alb (g/dl)	5.2 ± 0.2	4.9 ± 0.1**	5.0 ± 0.1*
T-Bil (mg/dl)	0.06 ± 0.01	0.05 ± 0.01*	0.04 ± 0.01**
Glucose (mg/dl)	130.6 ± 16.2	115.7 ± 11.1*	105.5 ± 10.4**
TG (mg/dl)	27.2 ± 7.5	15.3 ± 4.5**	25.3 ± 3.8
Phospholipid (mg/dl)	184.9 ± 19.5	164.8 ± 10.9*	247.9 ± 13.8**
TC (mg/dl)	108.2 ± 12.3	102.2 ± 6.9	186.0 ± 15.0**
BUN (mg/dl)	17.2 ± 2.7	17.9 ± 1.3	19.0 ± 2.0
CRN (mg/dl)	0.30 ± 0.03	0.31 ± 0.02	0.27 ± 0.02**
Na (mequiv./l)	144.1 ± 0.9	144.0 ± 1.3	143.4 ± 1.3
Cl (mequiv./l)	106.3 ± 1.9	107.0 ± 1.3	104.4 ± 1.5*
K (mequiv./l)	4.5 ± 1.7	4.0 ± 0.2	4.0 ± 0.2
Ca (mg/dl)	10.6 ± 0.5	10.3 ± 0.2	10.6 ± 0.1
IP (mg/dl)	6.7 ± 1.7	6.0 ± 0.6*	5.8 ± 0.3*
AST (IU/l)	82.7 ± 14.2	90.5 ± 5.1	115.1 ± 21.0**
ALT (IU/l)	42.6 ± 11.7	45.6 ± 3.7	61.7 ± 12.1**
ALP (IU/l)	343.6 ± 62.9	319.6 ± 33.4	350.9 ± 32.6

Abbreviations: TP, total protein; A/G, albumin/globulin ratio; Alb, albumin; T-Bil, total bilirubin; TG, triglyceride; TC, total cholesterol; BUN, blood urea nitrogen; CRN, creatinine; Na, sodium; Cl, chlorine; K, potassium; Ca, calcium; IP, inorganic phosphate; AST, aspartate aminotransferase; ALT, alanine aminotransferase; ALP, alkaline phosphatase.

[a] Mean ± SD.

* Significantly different from the controls at the levels of $p < 0.05$ (Dunnett's test).

** Significantly different from the controls at the levels of $p < 0.01$ (Dunnett's test).

2.6. Immunohistochemical staining for GST-P and proliferating cell nuclear antigen (PCNA)

Immunohistochemical staining was performed using polyclonal antibodies against GST-P (1:1000 dilution; Medical and Biological Laboratories Co., Ltd., Nagoya, Japan), a marker of preneoplastic lesions in the rat liver, and monoclonal anti-mouse PCNA antibodies (1:100; Dako, Glostrup, Denmark) to evaluate cell proliferation activity using the avidin–biotin peroxidase complex (ABC) method. The numbers (/cm^2) and areas (mm^2/cm^2) of the GST-P-positive foci (>0.1 mm^2) and the total areas of each liver section were measured using an IPAP image analyzer (Sumika Technos, Osaka, Japan) (Watanabe et al., 1994). The numbers of PCNA-positive cells per 600–800 intact liver cells from ten different areas per animal were counted to give the PCNA-positive ratio.

2.7. Statistics

The data obtained from the measurements of body weight, food and water consumption, organ weights, hematology, serum biochemistry, 8-OHdG levels, GST-P positive foci, PCNA-LI, *gpt* MFs and Spi$^-$ MFs were expressed as mean ± SD. The significant differences between the control and treated groups were determined by Dunnett's multiple comparison test (Dunnet, 1955) after ANOVA. The significant differences in incidences of lesions in the histopathological examinations were evaluated using Fisher's exact probability test. p-Values of less than 0.05 were considered statistically significant in both analyses.

3. Results

3.1. General condition, body weight, food consumption

One female from the control group died during the experimental period. However, no changes related to the death were observed in this rat. No remarkable changes in general appearances were observed in the safrole-treated groups during the experimental period. However, there was a marked suppression of body weight gain in the safrole-treated groups after week 2 (Fig. 1). Data for food consumption and safrole intake are summarized in Fig. 2 and Table 1. In both sexes, food consumption was decreased in the group given 0.5% safrole throughout the study, and the mean values for food consumption/animal were significantly lowered compared to the control group.

3.2. Hematology and serum biochemistry

The results of hematological measurements are shown in Table 2. White blood cell (WBC) counts and mean corpuscular hemoglobin (MCV) were significantly decreased and increased

Table 4
Organ weights in male F344 *gpt* delta rats given safrole for 13 weeks.

Groups No. of animal	Control 10	0.1% safrole 10	0.5% safrole 10
Body weight	369.5 ± 24.5[a]	341.1 ± 20.0**	264.4 ± 13.0**
Absolute (g)			
Liver	10.01 ± 0.80	9.90 ± 0.81	9.80 ± 0.86
Lungs	1.11 ± 0.07	1.06 ± 0.04	0.90 ± 0.06**
Kidneys	2.21 ± 0.13	2.14 ± 0.13	2.03 ± 0.12**
Brain	1.94 ± 0.07	2.00 ± 0.07	2.01 ± 0.35
Spleen	0.70 ± 0.05	0.66 ± 0.05	0.60 ± 0.05**
Thymus	0.24 ± 0.02	0.21 ± 0.02**	0.18 ± 0.02**
Heart	0.97 ± 0.06	0.88 ± 0.04**	0.72 ± 0.03**
Adrenals	0.045 ± 0.005	0.047 ± 0.004	0.048 ± 0.008
Testes	3.08 ± 0.16	3.10 ± 0.30	3.08 ± 0.14
Relative (g/100 g B.W.)			
Liver	2.71 ± 0.21	2.90 ± 0.15*	3.71 ± 0.37**
Lungs	0.30 ± 0.02	0.31 ± 0.01	0.34 ± 0.03**
Kidneys	0.60 ± 0.02	0.63 ± 0.03	0.77 ± 0.06**
Brain	0.53 ± 0.03	0.59 ± 0.02	0.76 ± 0.11**
Spleen	0.19 ± 0.01	0.19 ± 0.01	0.23 ± 0.02**
Thymus	0.07 ± 0.01	0.06 ± 0.01	0.07 ± 0.01
Heart	0.26 ± 0.01	0.26 ± 0.01	0.27 ± 0.02
Adrenals	0.012 ± 0.001	0.014 ± 0.001	0.017 ± 0.004**
Testes	0.84 ± 0.02	0.91 ± 0.06	1.17 ± 0.09**

[a] Mean ± SD.
* Significantly different from the controls at the levels of $p < 0.05$ (Dunnett's test).
** Significantly different from the controls at the levels of $p < 0.01$ (Dunnett's test).

respectively, in the treated groups of males. Conversely, significant increase of WBC counts was observed in the 0.5% group of females. In males, there was a significant decrease in red blood cell (RBC) counts and ratio of monocytes in the 0.5% group. In addition, significant increase of mean corpuscular hemoglobin (MCH) in the 0.5% group and decrease of platelet (Plt) counts in the 0.1% group were observed. In females, Plt counts and proportions of band form neutrophils, segmented neutrophils, eosinophils, reticulocytes showed significant decreases in the 0.5% group and proportions of lymphocytes showed significant increases in the treated group. In addition, a significant decrease of mean corpuscular volume (MCV) was observed in females of the 0.1% group.

Results from serum biochemical analysis are shown in Table 3. There were significant increases of aspartate (AST) and alanine aminotransferase (ALT) in both sexes in the 0.5% group. In males, significant increases of albumin (Alb), albumin/globulin (A/G) ratio, blood urea nitrogen (BUN), creatinine (CRN) and decreases of Glucose, triglyceride (TG), potassium (K), alkaline phosphatase (ALP) were observed in the 0.1% or 0.5% groups in a dose-dependent manner. In addition, significant increase of BUN, total cholesterol (TC) and calcium (Ca) and decrease of chlorine (Cl) were observed in males of the 0.5% group. In females, total protein (TP), albumin (Alb), total bilirubin (T-Bil), Glucose and inorganic phosphate (IP) were decreased in all treated groups. In addition, significant increase of TC and decrease of CRN and Cl were observed in the 0.5% group.

3.3. Organ weights and histopathological examination

Final body weights and the absolute and relative organ weights are shown in Tables 4 and 5. Final body weights were significantly decreased in the safrole-treated groups of both sexes. Absolute liver

Table 5
Organ weights in female F344 *gpt* delta rats given safrole for 13 weeks.

Groups No. of animal	Control 9	0.1% safrole 10	0.5% safrole 10
Body	202.1 ± 7.8[a]	168.7 ± 10.3**	150.1 ± 8.6**
Absolute (g)			
Liver	5.00 ± 0.42	4.62 ± 0.27**	5.65 ± 0.17**
Lungs	0.76 ± 0.03	0.73 ± 0.06	0.64 ± 0.04**
Kidneys	1.23 ± 0.06	1.13 ± 0.07*	1.09 ± 0.10**
Brain	1.82 ± 0.03	1.82 ± 0.08	1.76 ± 0.05
Spleen	0.43 ± 0.02	0.41 ± 0.02	0.40 ± 0.02**
Thymus	0.19 ± 0.01	0.18 ± 0.02	0.17 ± 0.02**
Heart	0.60 ± 0.02	0.53 ± 0.03**	0.45 ± 0.02**
Adrenals	0.052 ± 0.004	0.052 ± 0.005	0.046 ± 0.006**
Relative (g/100 g B.W.)			
Liver	2.48 ± 0.27	2.74 ± 0.10	3.77 ± 0.18**
Lungs	0.38 ± 0.03	0.44 ± 0.03**	0.43 ± 0.03**
Kidneys	0.61 ± 0.04	0.67 ± 0.02**	0.73 ± 0.04**
Brain	0.90 ± 0.04	1.08 ± 0.04**	1.17 ± 0.04**
Spleen	0.21 ± 0.01	0.25 ± 0.02**	0.26 ± 0.03**
Thymus	0.10 ± 0.01	0.11 ± 0.01	0.11 ± 0.02*
Heart	0.30 ± 0.02	0.31 ± 0.02	0.30 ± 0.01
Adrenals	0.026 ± 0.003	0.031 ± 0.002	0.030 ± 0.005

[a] Mean ± SD.
* Significantly different from the controls at the levels of $p < 0.05$ (Dunnett's test).
** Significantly different from the controls at the levels of $p < 0.01$ (Dunnett's test).

Table 6
Histopathological findings observed in F344 *gpt* delta rats given safrole for 13 weeks.

Organs	Findings	Sex	Male			Female		
		Groups	Control	0.1% safrole	0.5% safrole	Control	0.1% safrole	0.5% safrole
		No. of animals	10	10	10	9	10	10
Survival rate			100%	100%	100%	90%	100%	100%
Liver								
	Centrilobular vacuolar degeneration (large type)		1[a] (10[b])	6 (60)*	5 (50)	0 (0)	0 (0)	6 (60)**
	Single cell necrosis		1 (10)	9 (90)**	9 (90)**	4 (44)	7 (70)	6 (60)
	Centrilobular hepatocell hypertrophy		0 (0)	10 (100)**	10 (100)**	0 (0)	0 (00)	10 (100)**
	Microgranuloma		0 (0)	4 (40)*	2 (20)	0 (0)	1 (10)	2 (20)
Lung								
	Thrombus formation		3 (30)	1 (10)	1 (10)	0 (0)	0 (0)	1 (10)
	Focal hemorrhage		1 (10)	0 (0)	0 (0)	0 (0)	0 (0)	0 (0)
	Calcification		0 (0)	1 (10)	4 (40)*	0 (0)	0 (0)	0 (0)
	Foamy cell infiltration		0 (0)	1 (10)	1 (10)	1 (11)	1 (10)	1 (10)
	Inflammatory cell infiltration		0 (0)	0 (0)	1 (10)	0 (0)	0 (0)	0 (0)
	Arteritis		0 (0)	0 (0)	0 (0)	1 (11)	1 (10)	0 (0)
Kidney								
	Tubular hyaline droplets		0 (0)	0 (0)	10 (100)**	0 (0)	0 (0)	0 (0)
	Hyalin cast		0 (0)	2 (20)	3 (30)	0 (0)	0 (0)	0 (0)
	Tubular regeneration		1 (10)	9 (90)**	10 (100)**	0 (0)	0 (0)	0 (0)
	Granular cast		0 (0)	0 (0)	10 (100)**	0 (0)	0 (0)	0 (0)
	Pelvic calcification		0 (0)	0 (0)	10 (100)**	0 (0)	0 (0)	0 (0)
	Interstitial cell infiltration		0 (0)	0 (0)	6 (60)**	0 (0)	0 (0)	0 (0)
Heart								
	Myocardial inflammation		9 (90)	6 (60)	5 (50)	2 (22)	2 (20)	0 (0)
	Focal hemorrhage		0 (0)	1 (10)	0 (0)	0 (0)	0 (0)	0 (0)
Tongue								
	Inflammatory cell infiltration		1 (10)	2 (20)	3 (30)	0 (0)	1 (10)	0 (0)
Thyroid gland								
	Lymphoma		1 (10)	0 (0)	0 (0)	0 (0)	0 (0)	0 (0)
Parathyroid gland								
	Aberrant craniopharyngeal tissue		0 (0)	0 (0)	1 (10)	0 (0)	0 (0)	0 (0)
Pituitary gland								
	Anterior hyperplasia		0 (0)	0 (0)	0 (0)	0 (0)	0 (0)	1 (10)
Stomach								
	Inflammatory cell infiltration		1 (10)	0 (0)	0 (10)	0 (0)	0 (0)	0 (0)
Glandular stomach								
	Inflammatory cell infiltration		0 (0)	1 (10)	0 (0)	0 (0)	0 (0)	0 (0)
	Papilloma		0 (0)	0 (0)	0 (0)	0 (0)	1 (10)	0 (0)
Pancreas								
	Inflammatory cell infiltration		1 (10)	0 (0)	0 (0)	0 (0)	0 (0)	0 (0)
	Acinar atrophy		1 (10)	0 (0)	1 (10)	0 (0)	0 (0)	0 (0)
	Nesidioblastosis		0 (0)	0 (0)	0 (0)	0 (0)	1 (10)	0 (0)
Testis								
	Atrophy		0 (0)	1 (10)	0 (0)	–	–	–
Prostate gland								
	Prostatitis		0 (0)	1 (10)	0 (0)	–	–	–
Uterus								
	Extension		–	–	–	1 (11)	0 (0)	0 (0)
Deferent duct								
	Inflammatory cell infiltration		0 (0)	0 (0)	1 (10)	0 (0)	0 (0)	0 (0)
Bladder								
	Hydrops		0 (0)	0 (0)	1 (10)	0 (0)	0 (0)	0 (0)
Spinal cord cervical								
	Swelling of nerve cells		0 (0)	0 (0)	0 (0)	1 (11)	0 (0)	0 (0)

-, not examined.
[a] The number of animals with histopathological lesions.
[b] The incidence (%) of histopathological lesions.
* Significantly different from the controls at the levels of $p < 0.05$ (Dunnett's test).
** Significantly different from the controls at the levels of $p < 0.01$ (Dunnett's test).

veights in the 0.5% group of females and relative liver weights in he treated groups of males and in the 0.5% group of females signif-cantly increased. In males, absolute weights of the lungs, kidneys, pleen, thymus and heart were statistically lower in the 0.5% group ompared to the control group. In addition, a significantly decrease vas observed in the thymus and heart of the 0.1% group as well. On he contrast, relative weights of the lungs, kidneys, brain, spleen, drenals and testes were significantly increased in the 0.5% group ompared to the control group. In females, significant decrease of ıe absolute weights of the lungs, spleen, thymus and adrenals were bserved at the 0.5% group. But, the relative weights of these organs /ere significantly increased except for the adrenals. Furthermore, the absolute weights of the heart and kidneys were significantly decreased and relative weights of the brain and kidneys were significantly increased in the treated groups.

The results of histopathological examinations are shown in Table 6. Histopathologically, the incidence of centrilobular hypertrophy of hepatocytes was significantly increased in males of the treated groups and females in the 0.5% group compared with that in the control group (Fig. 3). Furthermore, in males, the single cell necrosis in the treated groups was significantly increased compared with that in the control group. The significant increase of centrilobular vacuolar degeneration was observed in males in the 0.1% group and in females in the 0.5% group. The incidences

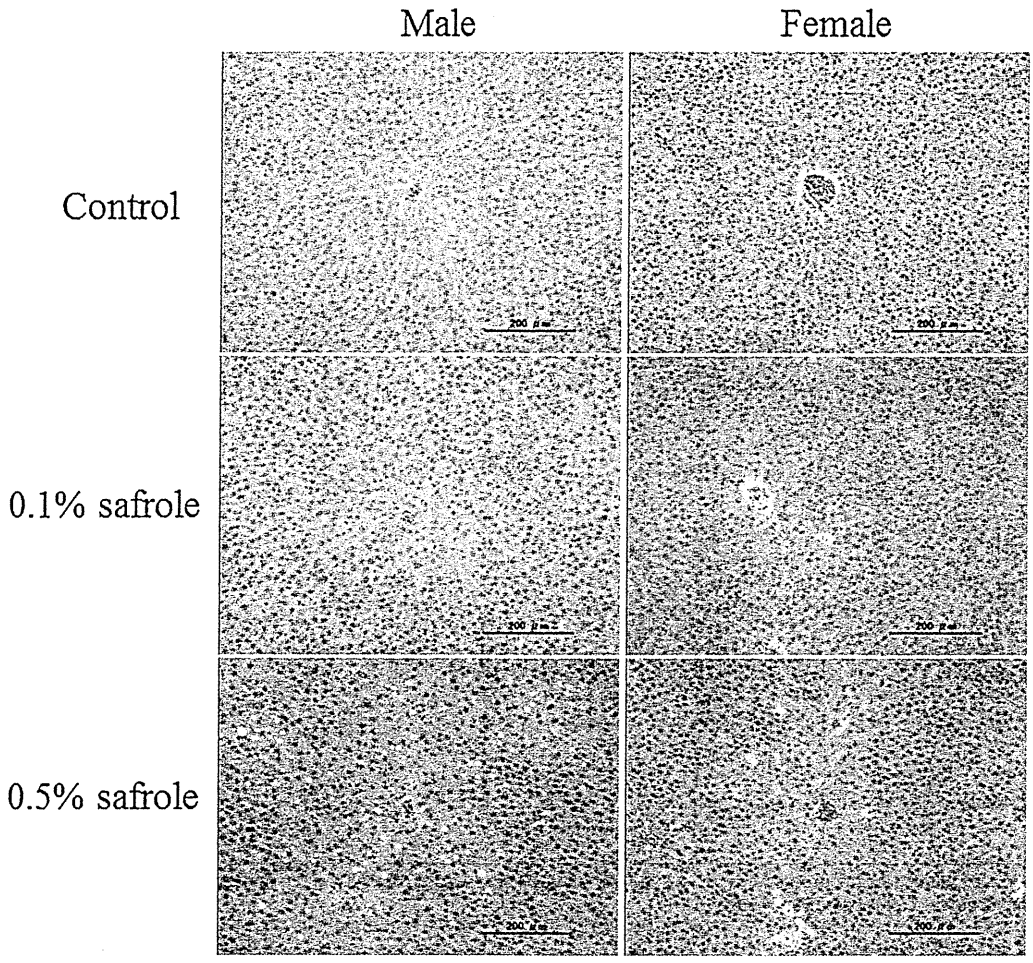

Fig. 3. Histopathological features in the livers of F344 *gpt* delta rats given safrole for 13 weeks. Centrilobular hypertrophy and vacuolar degeneration of hepatocytes are evident in the safrole-treated rats. HE stain. Bar represents 200 μm.

of tubular hyaline droplets, granular cast, pelvic calcification and interstitial cell infiltration of the kidney and of calcification of the lung were significantly increased in the males of the 0.5% groups. In addition, tubular regeneration of the kidney was significantly increased in the males of the all treated groups. On the other hand, thrombus formation and foamy cell infiltration of the lung, hyaline cast of the kidney, myocardial inflammation of the heart, and inflammatory cell infiltration of the tongue were observed in the treated rats without significant differences from the control group (10–60%).

3.4. *In vivo mutation assays in the livers*

Data for *gpt* and Spi$^-$ MFs in the liver of male and female *gpt* delta rats treated with safrole for 13 weeks are summarized in Tables 7 and 8, respectively. A significant increase of the *gpt* MFs was observed in males of the 0.5% (carcinogenic dose) group. In addition, increased *gpt* MFs were observed in females of the 0.5% group, although the increase was not statistically significant. There were no significant differences in the Spi$^-$ MFs among the groups in either sex. In the *gpt* mutant spectra, the predominant type of AT:GC transition was significantly induced by safrole (Table 9).

3.5. *Oxidative DNA damage in the liver*

In order to evaluate whether the oxidative damages to the cellular components occur during the formation of preneoplastic foci, the 8-OHdG levels were measured in liver DNA. The 8-OHdG levels in liver DNA were significantly increased in both sexes of the safrole-treated groups in a dose-dependent manner compared to those of the control groups (Table 10).

3.6. *Effects of safrole treatment on GST-P positive foci and cell proliferation*

Safrole treatment increased both the number and the area of GST-P positive foci in a dose-dependent manner compared with the control groups, although the differences were not statistically significant in males in the 0.1% group (Table 10). In addition, the effect of safrole on cell proliferation was evaluated by immunohistochemistry for PCNA (Table 10). The PCNA-positive ratio of hepatocytes was significantly increased in males of the treated groups and in females of the 0.5% group.

4. Discussion

A marked suppression of body weight gain was observed in the safrole-treated groups from week 2 to the end of the experiment. In serum biochemical examinations, there were significant increases of AST and ALT in both sexes of the 0.5% group. BUN and CRN levels significantly increased in males of the 0.5% group. In histopathological examinations, the incidences of centrilobular hypertrophy, centrilobular vacuolar degeneration and single cell necrosis of hepatocytes were significantly increased in males of the treated groups and in females of the 0.5% group. Furthermore, the incidences of tubular hyaline droplets, tubular regeneration, granular cast, pelvic

Table 7
gpt MFs in livers of F344 *gpt* delta rats given safrole for 13 weeks.

Sex	Groups	Animal no.	Cm^R colonies ($\times 10^5$)	6-TG^R and Cm^R colonies	Mutant frequency ($\times 10^{-5}$)	Mean ± S.D.
Male	Control	1	5.3	0	0.00	0.26 ± 0.21
		2	5.0	2	0.40	
		3	8.6	4	0.47	
		4	10.4	2	0.19	
		5	1.9	3	1.59[a]	
	0.1% safrole	11	6.3	4	0.63	0.77 ± 0.63
		12	4.5	8	1.76	
		13	5.3	5	0.95	
		14	4.7	1	0.21	
		15	7.2	2	0.28	
	0.5% safrole	21	3.4	7	2.05	1.89 ± 0.67**
		22	2.6	7	2.68	
		23	4.0	4	1.10	
		24	4.8	7	1.45	
		25	4.4	10	2.29	
Female	Control	36	6.9	7	1.01	0.65 ± 0.39
		37	4.9	3	0.62	
		38	5.1	0	0.00	
		39	7.7	7	0.90	
		40	5.6	4	0.71	
	0.1% safrole	46	6.2	9	1.46	0.98 ± 0.39
		47	7.6	10	1.32	
		48	12.8	10	0.78	
		49	5.3	3	0.57	
		50	7.9	6	0.76	
	0.5% safrole	56	2.8	3	1.06	1.26 ± 1.04
		57	3.3	3	0.91	
		58	3.6	2	0.56	
		59	3.2	10	3.09	
		60	3.0	2	0.66	

[a] Data of animal no. 5 was excluded for the calculation of the MF because of the poor packaging efficiency of the transgene (Smirnov–Grubbs test $T = 1.71$; $p < 0.05$).
** Significantly different from the control group at $p < 0.01$.

Table 8
Spi^- MFs in livers of F344 *gpt* delta rats given safrole for 13 weeks.

Sex	Groups	Animal no.	Plaques within XL-1 Blue MRA ($\times 10^5$)	Plaques within XL-1 Blue MRA (P2)	Mutant frequency ($\times 10^{-5}$)	Mean ± S.D.
Male	Control	1	9.5	9	0.94[a]	0.23 ± 0.51
		2	10.9	2	0.18	
		3	10.0	3	0.30	
		4	9.2	2	0.22	
		5	9.7	2	0.21	
	0.1% safrole	11	5.3	4	0.19	0.32 ± 0.25
		12	6.9	0	0.00	
		13	6.9	2	0.29	
		14	8.1	4	0.49	
		15	12.6	8	0.64	
	0.5% safrole	21	4.9	1	0.21	0.39 ± 0.29
		22	5.7	5	0.88	
		23	7.9	3	0.38	
		24	6.8	1	0.15	
		25	6.0	2	0.33	
Female	Control	36	7.1	1	0.14	0.36 ± 0.22
		37	6.7	3	0.45	
		38	9.8	1	0.10	
		39	8.3	4	0.48	
		40	11.5	7	0.61	
	0.1% safrole	46	6.9	0	0.00	0.21 ± 0.17
		47	7.4	1	0.14	
		48	11.4	5	0.44	
		49	7.1	1	0.14	
		50	9.5	3	0.31	
	0.5% safrole	56	2.5	2	0.79	0.29 ± 0.35
		57	5.3	0	0.00	
		58	6.0	1	0.17	
		59	6.0	3	0.50	
		60	8.7	0	0.00	

[a] Data of animal no. 1 was excluded for the calculation of the MF because of the poor packaging efficiency of the transgene (Smirnov–Grubbs test $T = 1.77$; $p < 0.05$).

Table 9
Mutation spectra of *gpt* mutant colonies in the livers of F344 *gpt* delta rats given safrole for 13 weeks.

Sex	Base substitution	Control		0.1% safrole		0.5% safrole	
		Number (%)	Mutation frequency (10^{-5})	Number (%)	Mutation frequency (10^{-5})	Number (%)	Mutation frequency (10^{-5})
Male	Transversions						
	GC-TA	2[a] (25.0)	0.06 ± 0.12	4(20.0)	0.15 ± 0.21	6(17.1)	0.30 ± 0.30
	GC-CG	1(12.5)	0.05 ± 0.09	2(10.0)	0.09 ± 0.20	4(11.4)	0.26 ± 0.31
	AT-TA	0	0	2(10.0)	0.07 ± 0.10	5(14.3)	0.29 ± 0.33
	AT-CG	0	0	0	0	1(2.9)	0.08 ± 0.17
	Transitions						
	GC-AT	4(50.0)	0.11 ± 0.12	8(40.0)	0.30 ± 0.25	5(14.3)	0.19 ± 0.18
	AT-GC	0	0	3(15.0)	0.12 ± 0.17	10(28.6)	0.54 ± 0.40**
	Deletion						
	Single bp	1(12.5)	0.05 ± 0.10	1(5.0)	0.04 ± 0.10	4(11.4)	0.19 ± 0.21
	Over 2 bp	0	0	0	0	0	0
	Insertion	0	0	0	0	0	0
	Complex	0	0	0	0	0	0
	Total	8	0.26 ± 0.21	20	0.77 ± 0.63	35	1.89 ± 0.67
Female	Transversions						
	GC-TA	4(19.0)	0.11 ± 0.19	10(26.3)	0.27 ± 0.17	5(25.0)	0.33 ± 0.45
	GC-CG	3(14.3)	0.08 ± 0.12	2(5.7)	0.04 ± 0.06	1(5.0)	0.06 ± 0.13
	AT-TA	1(4.8)	0.04 ± 0.09	6(15.8)	0.18 ± 0.19	2(10.0)	0.12 ± 0.28
	AT-CG	1(4.8)	0.04 ± 0.08	3(7.9)	0.08 ± 0.14	0	0
	Transitions						
	GC-AT	12(57.1)	0.38 ± 0.22	8(21.1)	0.18 ± 0.15	6(15.0)	0.37 ± 0.34
	AT-GC	0	0	8(21.1)	0.21 ± 0.05	5(25.0)	0.31 ± 0.31
	Deletion						
	Single bp	0	0	1(2.6)	0.03 ± 0.06	1(5.0)	0.07 ± 0.15
	Over 2 bp	0	0	0	0	0	0
	Insertion	0	0	0	0	0	0
	Complex	0	0	0	0	0	0
	Total	21	0.65 ± 0.39	38	0.98 ± 0.39	20	1.26 ± 1.04

[a] Number of colonies with independent mutations.
** Significantly different from the control group at $p < 0.01$.

calcification and interstitial cell infiltration in the kidney were significantly increased in males of the treated groups. The overall data indicated that safrole is a nephrotoxicant as well as a hepatotoxicant. In previous studies, the suppression of body weight gain and liver enlargement were also observed in safrole-treated rats (Homburger et al., 1962; Hagan et al., 1965). These results show that the *gpt* delta rat has a similar sensitivity to safrole in comparison to non-transgenic wild rats. This implies that the *gpt* delta rat model can be used to investigate general toxicities of agents.

Safrole forms safrole-specific DNA adducts through hepatic cytochrome P450 biotransformation and subsequent conjugation by sulfotransferase (Miller and Miller, 1983). Alternatively, safrole can be biotransformed though the methylenedioxy ring-opening to hydroxychavicol. Hydroxychavicol could be biotransformed to o-quinone through 2-electron oxidation, and this redox-active quinone is considered to induce oxidative damages (Klungsoyr and Scheline, 1983; O'Brien, 1991). In fact, the levels of 8-OHdG were significantly increased in both sexes of the safrole-treated groups as compared to those of the control group. To the best of our knowledge, there are no reports demonstrating the significant increase of 8-OHdG levels in livers of rats treated with a low dose (half of a carcinogenic dose) for 13 weeks. However, the genotoxicity of safrole remained unknown in conventional genotoxicity tests such as the Ames test, sister chromatid exchanges (SCE) test and micronucleus test in spite of its hepatocarcinogenicity being clear (Green and Savage, 1978; Swanson et al., 1979; Baker and Bonin, 1985; Bradley, 1985; Gocke et al., 1981). The present study demonstrated that an increase or increasing tendency of the *gpt* MFs was observed in both sexes in the 0.5% group, a carcinogenic dose, despite the Spi$^-$ MFs being unchanged. These results suggested that safrole has a potential to be genotoxic *in vivo* in the livers of rats. In the mutation spectra, the AT:GC transitions were significantly induced by safrole in males of the 0.5% group. If has been reported that 8-OHdG is capable to form a base pair with adenine and subsequently produce a GC:AT transversion mutation. In addition, recent studies suggest that 8-OHdG can cause large deletion mutations associated with double strand break during base excision repair by *OGG1* (Umemura

Table 10
8-OHdG, PCNA and GST-P levels in the livers of F344 *gpt* delta rats given safrole for 13 weeks.

Sex	Treatment	Control	0.1% safrole	0.5% safrole
Male	8-OHdG	0.27 ± 0.02[a]	0.35 ± 0.05*	0.52 ± 0.06**
	PCNA-positive ratio	0.27 ± 0.12	0.54 ± 0.17*	0.51 ± 0.14*
	GST-P (number/cm^2)	0.00 ± 0.00	0.88 ± 0.55	9.42 ± 3.51**
	GST-P (mm^2/cm^2)	0.00 ± 0.00	0.005 ± 0.004	0.134 ± 0.070**
Female	8-OHdG	0.36 ± 0.04	0.51 ± 0.06**	0.62 ± 0.06**
	PCNA-positive ratio	0.20 ± 0.07	0.66 ± 0.09	1.06 ± 0.55**
	GST-P (number/cm^2)	0.00 ± 0.00	0.44 ± 0.46*	2.78 ± 1.22**
	GST-P (mm^2/cm^2)	0.00 ± 0.00	0.004 ± 0.005	0.026 ± 0.016**

[a] Mean ± SD.
* Significantly different from the controls at the levels of $p < 0.05$ (Dunnett's test).
** Significantly different from the controls at the levels of $p < 0.01$ (Dunnett's test).